

Chapter 1

Introduction

In the future, multimedia communications will be the main stream of wireless communication systems and realizing effective multi-rate physical-layer transmission becomes a highly challenging research in the current development of high speed wireless communications. The 3rd Generation Partnership Project has initiated standardization of High-Speed Downlink Packet Access (HSDPA) [1] for the Wideband direct sequence Code Division Multiple Access (W-CDMA) in the forward link [2], to support packet data services with higher than 2-Mbps throughput. However, in order to achieve much higher throughput in the system beyond IMT-2000, such as a peak throughput above 100Mbps in the forward link, DS-SS-CDMA technique will suffer from more hostile fading channels, so an entirely new wireless access scheme is required.

Recent years, some new transmission methods based on the combination of code division multiple access (CDMA) and orthogonal frequency division multiple access (OFDM) are proposed [3-5]. These transmission methods retain the advantages from both CDMA and OFDM techniques, such as high and soft-limited user capacity and robustness to multi-path fading channels. This is because OFDM mitigate the degradation due to severe inter-symbol interference by using many low symbol rate sub-carriers, and inserting a cyclic extension. Furthermore, it mitigates the difficulty of equalization for frequency-selective faded wideband CDMA signals by converting a frequency selective channel into a number of parallel flat fading channels.

MC-CDMA and MC-DS-CDMA are two main types of conventional OFDM-CDMA systems. MC-CDMA systems combine MC modulation and frequency domain spreading. A data symbol is replicated into several parallel copies. Each copy is multiplied by a chip from a spreading code and modulates a different carrier frequency. In contrast, MC-DS-CDMA systems combine MC modulation and time domain spreading, where a data sequence is spread in the time domain by a given spreading code and then modulates multiple sub-carriers in different OFDM-CDMA symbols. These two schemes are called 1-D OFDM-CDMA systems, since the data is just spread in time domain or frequency domain.

In the thesis, we propose an adaptive OFDM-CDMA system with two dimensional spreading in the forward link, which is originally based on MC-CDMA or MC-DS-CDMA exhibits more flexible characteristics than conventional one dimensional spreading Multi-carrier CDMA systems. Furthermore, 2-D OFDM-CDMA [6] has many advantages because it makes finer partition of system resource into time, frequency, and code domain, which contributes to efficient resource utilizations. Some papers propose 2D OFDM-CDMA systems just based on DS-CDMA [7], [8]. Without OFDM modulation, the system still need for a RAKE receiver to resolve the time-dispersive channel. NTT DoCoMo proposed some design ideas for 2-D OFDM-CDMA systems [9-11], called variable spreading factor-orthogonal frequency and code division multiplexing (VSF-OFCDM) which means changing the spreading factors according to the cell structure, radio link conditions, and radio link parameters. They suggest not performing chip-interleaving in both time and frequency domain and prioritizing time domain spreading rather than frequency domain spreading in order to maintain code orthogonality [12]. It should be noted that the overall received signal quality employing two-dimensional spreading

through a multi-path fading channel depends on the tradeoff relation between the increasing frequency diversity effect and the impairment of code orthogonality. Their design idea is slanted in favor of reducing MAI at the cost of losing diversity gain. We think the diversity should not be neglected. As a result, it is very important to take both MAI and diversity into account for the optimum design.

We find that some factors would influence the compromise between MAI and diversity based on propagation channel conditions and transmitting user numbers. Mostly, to obtain the optimal performance, we should jointly take all relevant factors into account at one time while designing adaptive 2D OFDM-CDMA systems. The relevant factors that can be adaptively controlled include: the spreading patterns on which spreading chips are mapped, allocation methods for time/frequency resource, spreading code assignment for simultaneous users, and the diversity combining schemes employed in the receiver side.

It is emphasized that unlike NTT DoCoMo systems, we propose many combining schemes including single user detection and multi-user detection to get more flexible systems and better performance. Conventional multi-carrier single user combining methods include EGC, MRC and MMSE [2]. We investigate the characteristics of these schemes working on our adaptive 2D OFDM-CDMA systems. Furthermore, considering the performance of single user detection is not satisfactory, we also propose new multi-user detection methods to achieve optimum performance. The MMSE/PIC scheme is designed for receiver side, and pre-weight allocation method is used in the transmitter side.

The rest of this thesis is organized as follows. In Chapter 2, we introduce the general idea of OFDM, CDMA and Multi-carrier CDMA. Then we describe the transmitter and receiver structure for 2D OFDM-CDMA systems and simulation configuration. In Chapter 3, the adaptive allocation design of 2D OFDM-CDMA systems is discussed. Chapter 4 explains the single user detection methods, followed by Chapter 5, which proposes new multi-user combining schemes. Finally, we give conclusions and discussions in Section 6.

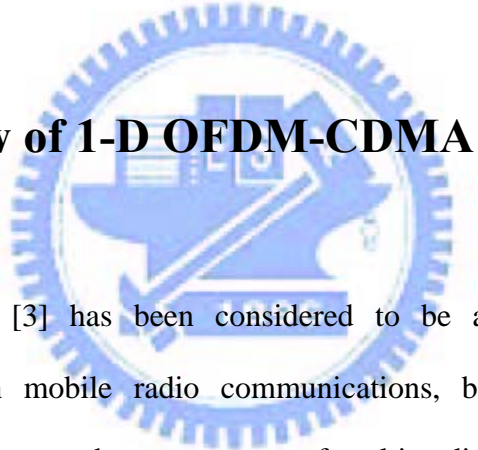


Chapter 2

2-D OFDM-CDMA Systems

In this chapter, we mainly introduce our 2-D OFDM-CDMA systems. At first, we introduce conventional 1-D OFDM-CDMA systems in Section 2.1, which consists of the concept of OFDM, CDMA, MC-CDMA and MC-DS-CDMA techniques. Then we propose the transmitter and receiver structures for 2-D OFDM-CDMA systems. Finally, the simulation configuration is described.

2.1 Overview of 1-D OFDM-CDMA Systems



CDMA technique [3] has been considered to be a candidate to support multimedia services in mobile radio communications, because it has its own capabilities to cope with asynchronous nature of multimedia data traffic, to provide higher capacity over conventional access techniques such as time-division multiple access (TDMA) and frequency-division multiple access (FDMA), and to combat the hostile channel frequency selectivity.

Recently, a new CDMA system based on a combination of CDMA scheme and orthogonal frequency division multiplexing (OFDM) signaling, OFDM-CDMA or Multi-carrier CDMA [3-5], has drawn a lot of attention in the field of radio communication. This is mainly because the signal can be easily transmitted and received using the fast Fourier transform (FFT) device without increasing the

transmitter and receiver complexities and it is potentially robust to channel frequency selectivity with good frequency utilization efficiency.

The Multi-carrier CDMA schemes are categorized mainly into two groups. One is MC-CDMA, which spreads the data in the frequency domain, and the other is MC-DS-CDMA, which spreads the data in the time domain.

2.1.1 DS - CDMA

The DS-CDMA transmitter spreads the original data stream using a given spreading code in the time domain. The capability of suppressing multi-user interference is determined by the cross-correlation characteristic of the spreading codes. Also, a frequency selective fading channel is characterized by the superimposition of several signals with different delays in the time domain. Therefore, the capability of distinguishing one component from other components in the composite received signal is determined by the auto-correlation characteristic of the spreading codes.

Fig.2.1 shows the DS-CDMA transmitter of the j -th user for binary phase shift keying/coherent detection (CBPSK) scheme and the power spectrum of the transmitted signal, respectively, where G_{DS} denotes the processing gain and $c^j(t) = [c_1^j c_2^j \dots c_{G_{DS}}^j]$ the spreading code of the j -th user.

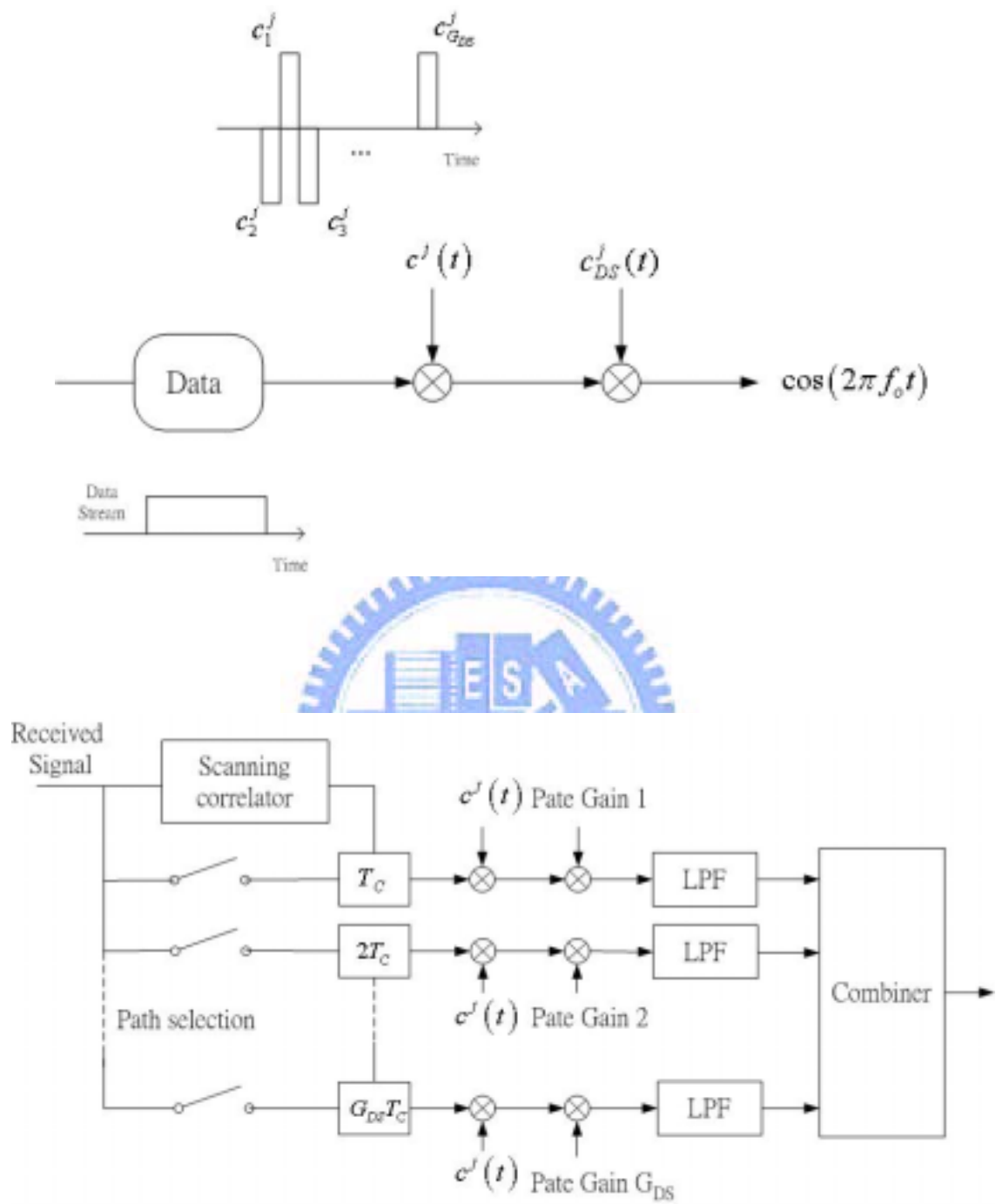


Fig 2.1 The transmitter and receiver of DS-SS systems

2.1.2 OFDM

The principle of OFDM is to divide the transmission channel into a number of orthogonal sub-carriers. The high rate symbols are transformed into low rate symbols in the Fig.2.2 and serial data stream is divided into several parallel streams and each is modulated using a sub-carrier.

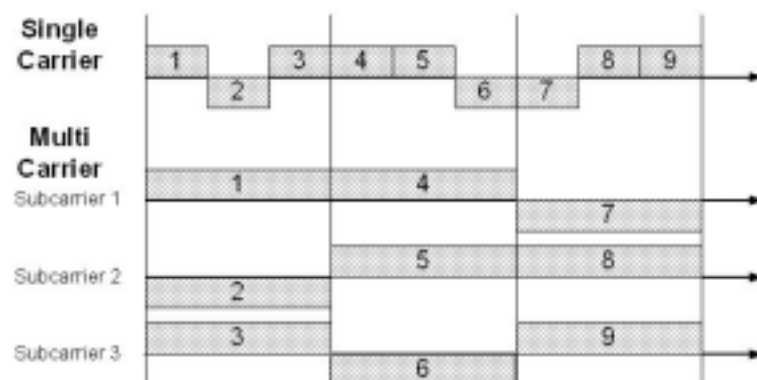


Fig. 2.2 Single-carrier and multi-carrier transmission

In a single carrier channel, symbols are transmitted sequentially with each data symbol occupying the entire available bandwidth. Single channel communication is usually far more susceptible to inter symbol interference than multi-carrier modulation. In the OFDM, since the entire channel bandwidth is divided into several narrow sub-bands, the frequency response over each individual sub-band is relatively flat. Each sub-channel occupies only a small fraction of the original bandwidth. Therefore OFDM can resist frequency selective fading channel and inter-symbol interference.

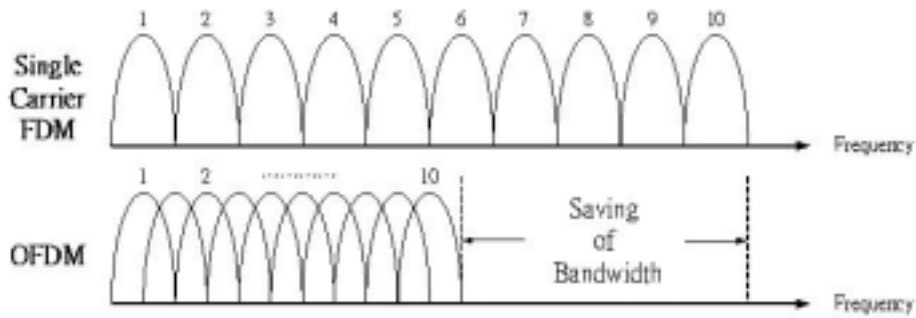


Fig .2.3 Bandwidth efficiency of OFDM and conventional FDM

OFDM is the special case of conventional multi-carrier modulation where its carrier spacing is selected so that each sub-carrier is orthogonal to the other carriers as shown in the Fig. 2.3., and the time domain signals can be represented as the sum of orthogonal sine waves in the Fig. 2.4.

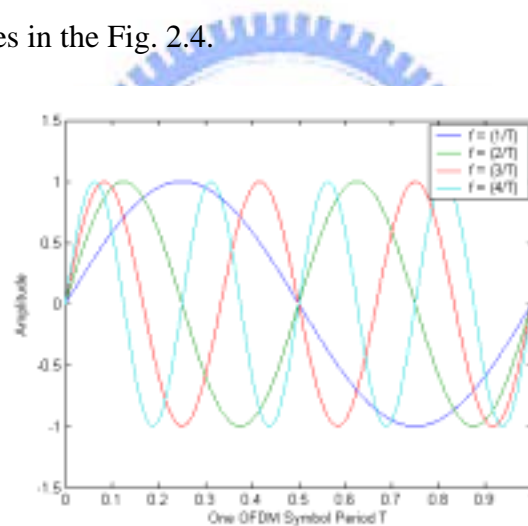


Fig.2.4 OFDM symbols in the time domain

Fig. 2.5 shows the analog transmitter of OFDM systems. Each data is modulated on a sub-carrier and OFDM symbol is formed by the sum of total sub-carriers. Fig. 2.6 shows the receiver of OFDM systems. The received signal is integrated to detect the data. Recently, discrete time implementations were proposed based on DFT. Fast Fourier transform (FFT) contributed to a great extent in reducing the implantation complexity.

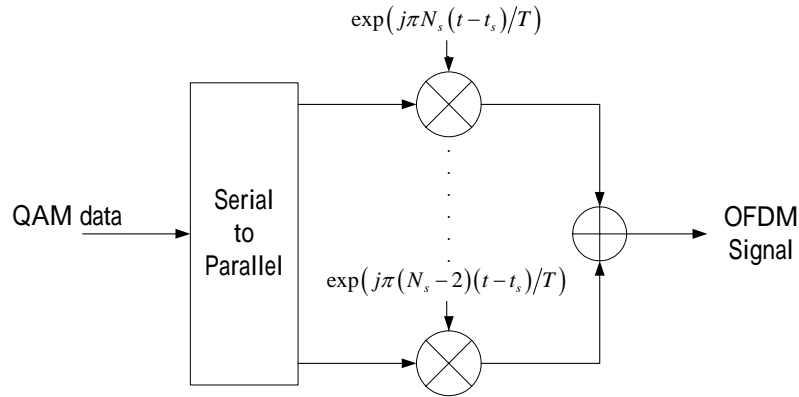


Fig. 2.5 The analog transmitter of OFDM systems

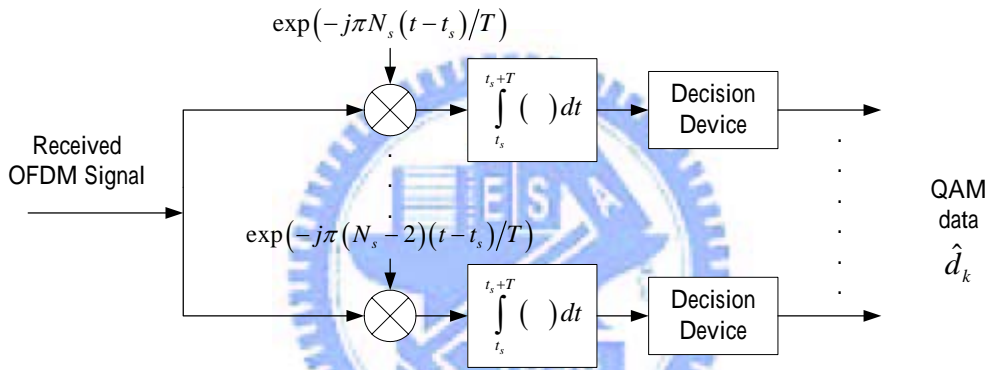


Fig. 2.6 The analog receiver of OFDM systems

In the transmitter, after IFFT processing, the OFDM symbol should add guard interval which is the copy of the last part in order to avoid the inter-symbol interference (ISI) and inter-carrier interference (ICI).

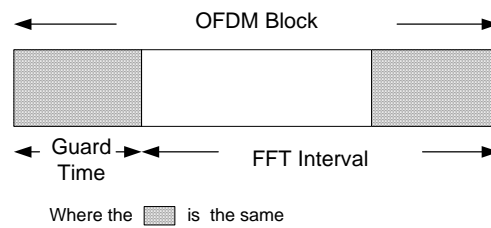


Fig. 2.7 The guard interval of OFDM symbols

2.1.3 MC-CDMA

The MC-CDMA transmitter spreads the original signal using a given spreading code in the frequency domain. In other words, a fraction of the symbol corresponding to a chip of the spreading code is transmitted through a different sub-carrier. For MC transmission, it is essential to have frequency nonselective fading over each sub-carrier. In a downlink mobile radio communication channel, we can use the OVSF codes as an optimum orthogonal set, because we do not have to pay attention to the auto-correlation characteristic of the spreading codes.

MC-CDMA scheme is discussed assuming that the number of sub-carriers and the processing gain are all the same. However, we do not have to choose $N_C = G_{MC}$. Figure 2.8 shows the MC-CDMA transmitter and receiver of the j -th user for BPSK scheme and the power spectrum of the transmitted signal, respectively, where G_{MC} denotes the processing gain, N_C the number of sub-carriers, and $c^j(t) = [c_1^j c_2^j \dots c_{G_{MC}}^j]$ the spreading code of the j -th user. If the original symbol rate is high enough to become subject to frequency selective fading. The signal needs to be first S/P-converted before spreading over the frequency domain. This is because it is crucial for multi-carrier transmission to have frequency non-selective fading over each sub-carrier. Figure shows the modification to ensure frequency non-selective fading, where T_s denotes the original symbol duration, and the original data sequence is first converted into P parallel sequences, and then each sequence is mapped onto G_{MC} sub-carriers ($N_C = P \times G_{MC}$).

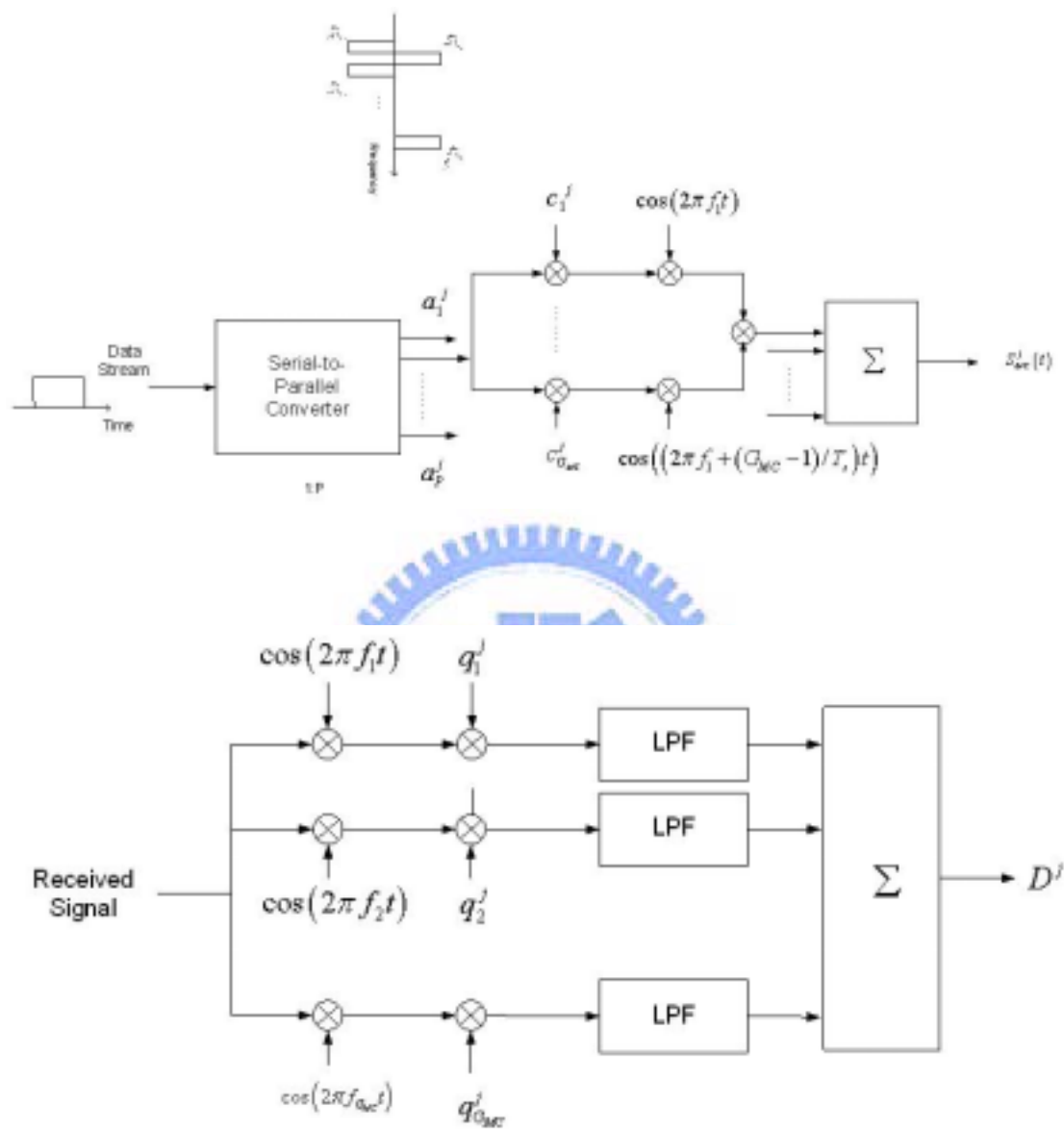


Fig 2.8 The transmitter and receiver of MC-CDMA systems

2.1.4 MC-DS-CDMA

Multi-carrier DS-CDMA transmitter spreads the S/P converted data streams using a given spreading code in the time domain so that the resulting spectrum of each sub-carrier can satisfy the orthogonality condition with the minimum frequency separation. This scheme is originally proposed for an uplink communication channel, because the introduction of OFDM signaling into DS-CDMA scheme is effective for the establishment of a quasi-synchronous channel.

Figure 2.9 show the Multi-carrier DS-CDMA transmitter of the j -th user and the power spectrum of the transmitted signal, respectively, where G_{MD} denotes the processing gain, N_c the number of sub-carriers, and $c^j(t) = [c_1^j c_2^j \dots c_{G_{MD}}^j]$ the spreading code of the j -th user.

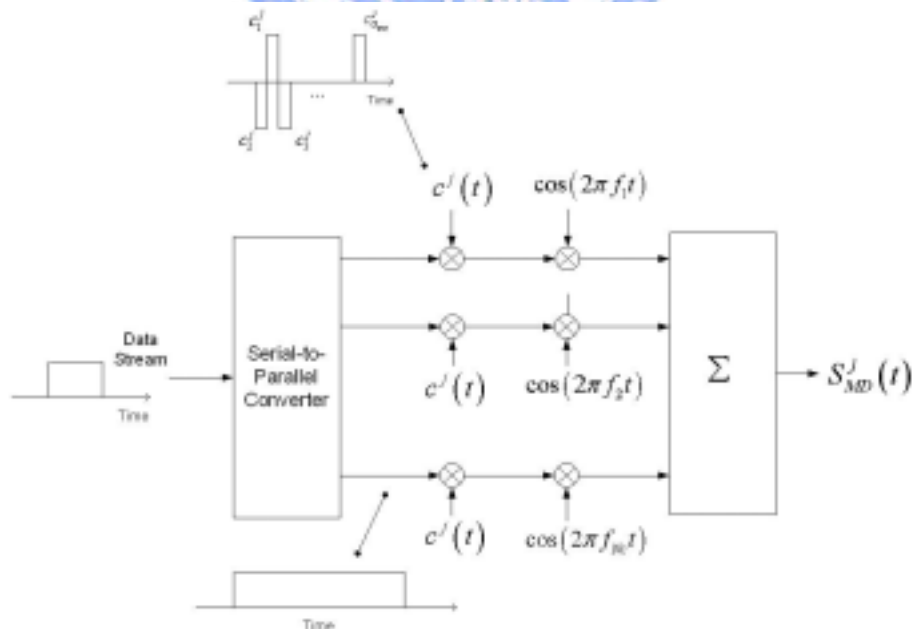


Fig 2.9 Multi-carrier DS-CDMA transmitter

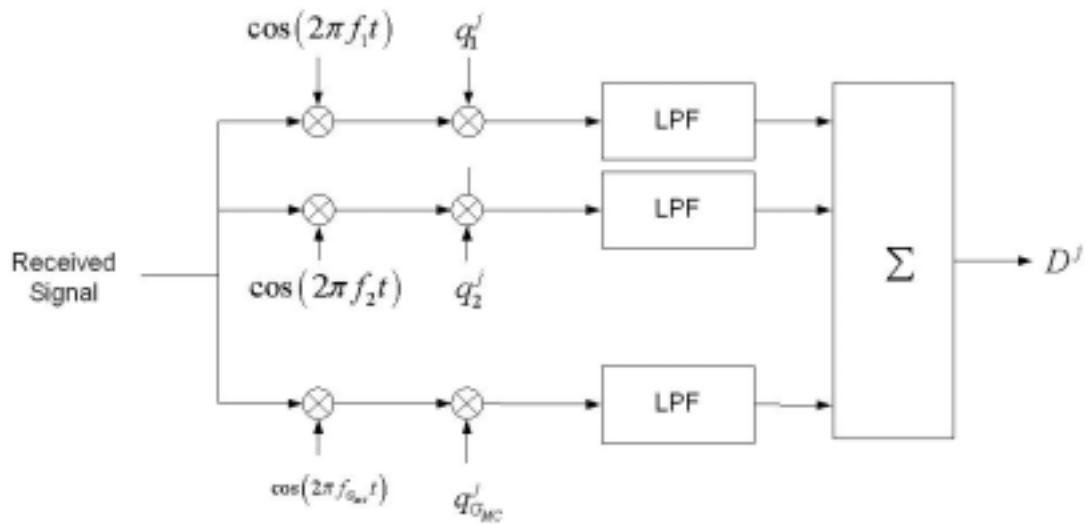


Fig 2.10 Multi-carrier DS-CDMA receiver



2.2 Architecture of 2-D OFDM-CDMA Systems

2.2.1 Transmitter model

We consider a 2-D OFDM-CDMA system where N_u users are transmitting simultaneously in a synchronous manner using OVSF orthogonal codes. The system corresponds to the forward link from the base station to the users. At the transmitter, the binary information data bits are modulated with QPSK modulation. After modulation, the data symbol is represented as d_p^u for the p th data symbol of u th user. We spread the data stream with the user's time domain spreading sequence $c^u = [c_1^u \ c_2^u \ \dots \ c_{G_T}^u]$, where G_T is the length of time domain spreading code. Then a chip data from the output of time domain spreading is replicated into G_F parallel copies, each of which is multiplied by a chip from the corresponding frequency domain spreading code $c^u = [c_1^u \ c_2^u \ \dots \ c_{G_F}^u]$, where G_F is the length of frequency domain spreading code. After two dimensional spreading, we perform the chip interleaving in order to get frequency diversity. The i th OFDM-CDMA block symbol for user u is formed by placing the resulting chips into $N > PG_F$ available sub-channels, each having width $\Delta f = 1/T_{FFT}$, by using an inverse fast Fourier transform (IFFT) of size N . In practice, N is larger than the number of sub-channels PG_F required for the transmission of the data in order to avoid frequency aliasing after sampling at the receiver. For that reason, the data vector at the input of the IFFT is padded with zeros at its edges so that the $(N - PG_F)$ unmodulated carriers are split in both sides of the useful spectrum. The function of the identical frequency

interleavers is to ensure that the G_F chips corresponding to each of the P symbols are transmitted over approximately independently faded sub-channels. This is possible if P/T_{FFT} is larger than the coherence bandwidth of the channel. After performing a parallel to serial conversion, a guard interval is added in the form of a cyclic prefix, and the signals of all the users are added and transmitted through the channel.

Fig. 2.11 shows the adaptive 2-D OFDM-CDMA transmitter block diagram. The length of G_F, G_T is decided based on the channel conditions and channel load. We will discuss the design issues in the next chapter.

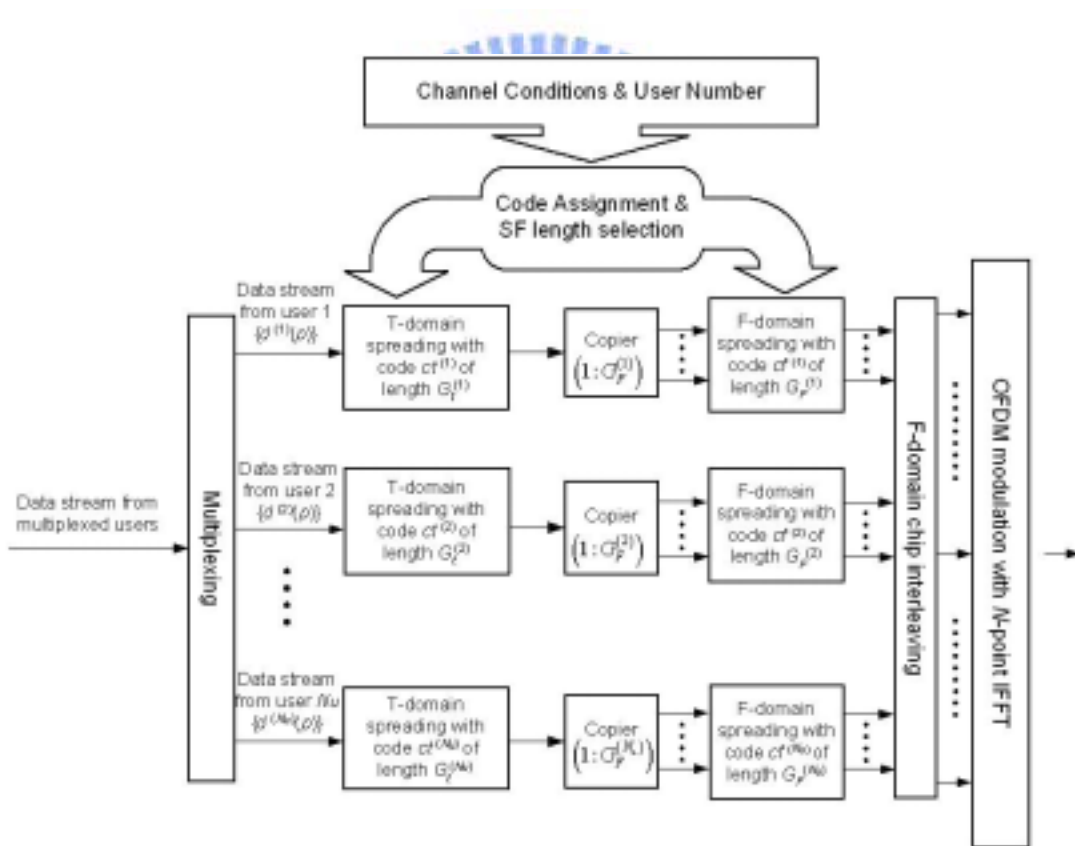


Fig. 2.11 The transmitter structure of adaptive 2-D OFDM-CDMA systems

Now we use the equations to explain the transmitting signals, the data of the k th sub-carrier is,

$$X_{k,j}^u = X_{i+p \cdot G_F, j}^u = d_p^u \cdot c f_i^u \cdot c t_j^u \quad (2.1)$$

- * p : user data symbol
- * u : user index
- * k : subcarrier index
- * i : spreading code index in frequency domain
- * j : OFDM symbol index (spreading code index in time domain)
- * G_T : SF length in time domain
- * G_F : SF length in frequency domain

Fig.2.12 shows the frequency domain spreading and time domain spreading process for the equation (2.1)

The n th IFFT output of the j th OFDM-CDMA block symbol is

$$x_{n,j} = \frac{1}{N} \sum_{u=1}^{N_u} \sum_{k=1}^K X_{k,j}^u \cdot e^{\frac{j2\pi kn}{N}} \quad (2.2)$$

The transmitted signal during the G_T th OFDM-CDMA block symbol period can be written as follows,

$$s(t) = \sum_{j=1}^{G_T} \sum_{n=-N_g}^{N-1} x_{n,j} \cdot g_T(t - nT_s - jN_{OFDM}T_s) \quad (2.3)$$

- * N_u : number of user
- * K : number of subcarrier for one OFDM symbol
- * $g_T(t)$: Transmit Filter

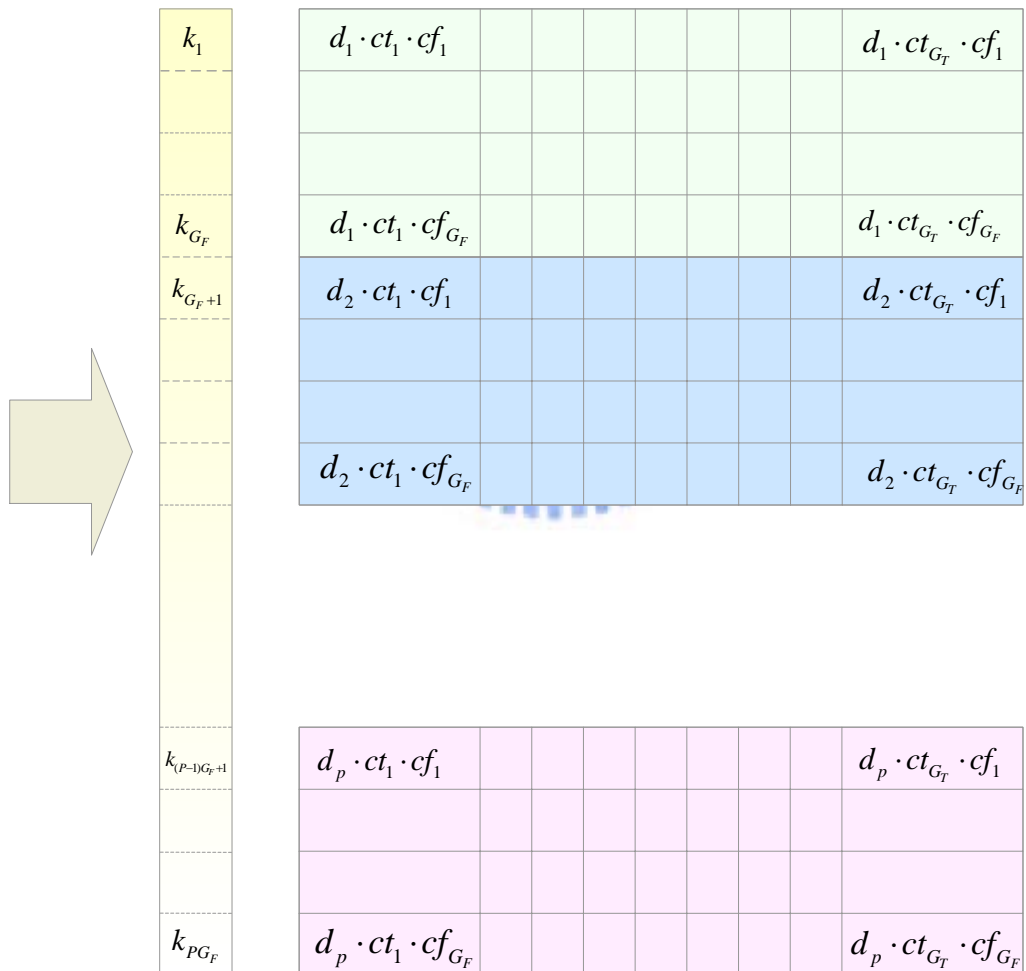
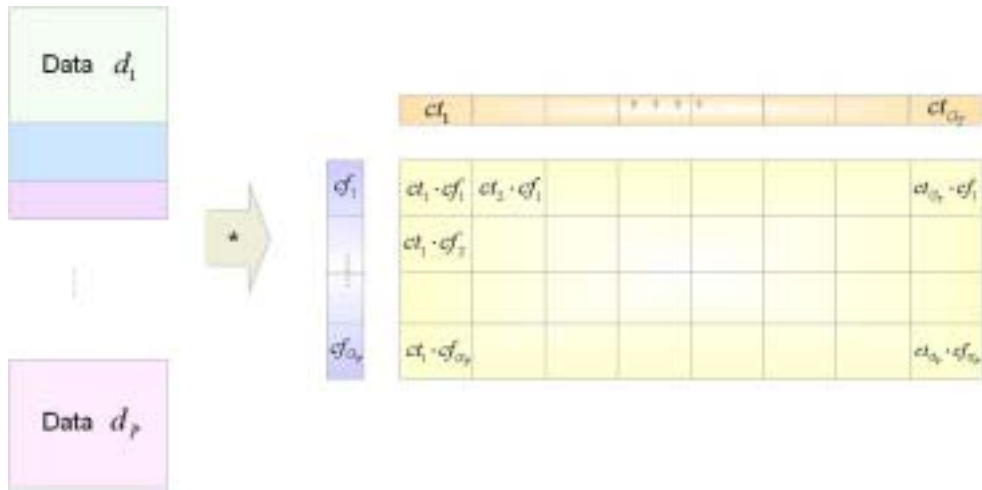


Fig. 2.12 The process of the time and frequency domain spreading

2.2.2 Orthogonal Spreading codes

We use OVSF codes or orthogonal Walsh-Hadamard (WH) codes for the downlink [14]. The generation of the WH codes is described as follows. We can begin with a basic matrix unit which is

$$\mathbf{H}_0 = \begin{bmatrix} 1 & 1 \\ 1 & -1 \end{bmatrix} \quad (2.4)$$

From (2.4), we can use a recursive procedure to generate a orthogonal matrix, \mathbf{H}_n , of size $2^{n-1} \times 2^{n-1}$ described as


$$\mathbf{H}_n = \begin{bmatrix} \mathbf{H}_{n-1} & \mathbf{H}_{n-1} \\ \mathbf{H}_{n-1} & -\mathbf{H}_{n-1} \end{bmatrix} \quad (2.5)$$

Each row of the matrix, \mathbf{H}_n , gives a possible code for a user. It can be easily shown that any two rows in the matrix \mathbf{H}_n are perfectly orthogonal. In other words, the cross-correlation is zero. The WH code is good for OFDM-CDMA applications. One constraint with the WH code is that the numbers to the orthogonal codes is equal to the code length.

2.2.3 Channel model

We assume a slow fading, multipath, Rayleigh channel whose impulse response has L path arrivals, which are described by independent zero-mean, complex Gaussian distributed path gain processes. We assume that the delay spread of the channel is shorter than the guard interval of the OFDM-CDMA symbol and the channel is time-invariant during the time spread duration.

The channel response is represented as

$$h(t; \tau) = \sum_{l=0}^{L-1} h_l(t) \delta(\tau - lD_{\text{exp}}T_s) \quad (2.6)$$

where $h_l(t)$ is the l -th path gain, which is a mutually independent complex Gaussian random process with zero mean and variance σ_l^2 , and $D_{\text{exp}}T_s$ is the inter-arrival time between two consecutive paths.

2.2.4 Receiver model

Because of the existence of a guard interval with duration at least equal to the delay spread of channels, there is no inter-symbol interference, and assume perfect synchronization. The received signal in the equivalent low-pass representation is given by

$$\begin{aligned}
r(t) &= s(t) \otimes h(t) \otimes g_R(t) + n(t) \otimes g_R(t) \\
&= \sum_{j=1}^{G_T} \sum_{n=-N_g}^{N-1} x_{n,j} f(t - nT_s - jN_{OFDM}T_s) + z(t)
\end{aligned} \tag{2.7}$$

- * $x_{n,j} = \frac{1}{N} \sum_{k=0}^{N-1} X_{k,j} e^{j2\pi kn/N}$: IFFT Output for j-th OFDM Symbol
- * $f(t) = g_T(t) \otimes h(t) \otimes g_R(t)$: Overall Impulse Response
- * $g_T(t)$: Transmit Filter
- * $h(t) = \sum_{l=0}^{L-1} h_l \delta(t - lT_{sa})$: Channel Impulse Response
- * $g_R(t)$: Receive Filter
- * $z(t) = n(t) \otimes g_R(t)$
- * $n(t)$: AWGN

The receiver structure for the reference user is illustrated in Fig.2.13. At the receiver side, the signals are first sampled and then the guard intervals are removed.

The sampled data is

$$\begin{aligned}
r(n, j) &= r(t) \Big|_{t=nT_s + jN_{OFDM}T_s} \\
&= y(n, j) + z(n, j) \quad n = 0, \dots, N-1
\end{aligned} \tag{2.8}$$

An FFT of size N is performed to resolve the desired sub-carrier components and frequency de-interleaving takes place. Assume that the maximum delay spread is shorter than the guard interval, and then the demodulated sequence after performing de-interleaving can be expressed as

$$\begin{aligned}
Y(k, j) &= DFT \{y(n, j)\} \quad k = 0, \dots, N-1 \\
&= \sum_{n=0}^{N-1} y_{n,j} e^{-\frac{j2\pi kn}{N}} \\
&= \sum_{n=0}^{N-1} \left[\frac{1}{N} \sum_{u=1}^{N_u} \sum_{k=0}^{N-1} X_{k,j}^u H_{k,j} \cdot e^{\frac{j2\pi kn}{N}} \right] \cdot e^{-\frac{j2\pi kn}{N}} \\
&= \sum_{u=1}^{N_u} \sum_{k=0}^{N-1} X_{k,j}^u H_{k,j} \\
&= \sum_{u=1}^{N_u} \sum_{k=0}^{N-1} X_{k,j}^u |H_{k,j}| \cdot e^{-j\theta_{k,j}} \\
&= \sum_{u=1}^{N_u} \sum_{p=1}^P \sum_{i=1}^{G_F} d_p^u \cdot cf_i^u \cdot ct_j^u \cdot |H_{i+p \cdot G_F, j}| \cdot e^{-j\theta_{i+p \cdot G_F, j}}
\end{aligned} \tag{2.9}$$

Following FFT demodulation, the frequency domain de-spreading is performed using the desired code cf^1 , and then the de-spreading components are weighted by their respective combining coefficients and summed up. After receiving the G_T OFDM-CDMA block symbols and performing frequency de-spreading respectively, the results are multiplied by time domain spreading codes to perform time domain de-spreading. Finally the decision part can be expressed as

$$\begin{aligned}
D_p^1 &= \sum_{i=1}^{G_F} \sum_{j=1}^{G_T} r_{i+p \cdot G_F, j} \cdot cf_i^1 \cdot ct_j^1 \cdot \alpha_{i+p \cdot G_F, j} e^{j\theta_{i+p \cdot G_F, j}} \\
&= \underbrace{d_p^1 \sum_{i=1}^{G_F} \sum_{j=1}^{G_T} |H_{i+p \cdot G_F, j}| \cdot \alpha_{i+p \cdot G_F, j}}_{\text{desired signal}} \\
&\quad + \underbrace{\sum_{u=2}^{N_u} \sum_{i=1}^{G_F} \sum_{j=1}^{G_T} d_p^u |H_{i+p \cdot G_F, j}| \cdot \alpha_{i+p \cdot G_F, j} \cdot cf_i^1 \cdot ct_j^1 \cdot cf_i^u \cdot ct_j^u}_{MAI} \\
&\quad + \underbrace{\sum_{i=1}^{G_F} \sum_{j=1}^{G_T} z_{i+p \cdot G_F, j} \cdot \alpha_{i+p \cdot G_F, j} \cdot cf_i^1 \cdot ct_j^1}_{\text{noise}}
\end{aligned} \tag{2.10}$$

* α_k : combining weight of the kth sub-carrier.

From the decision variable, we can find that the different performance is achieved according to different combining methods and spreading allocation methods.

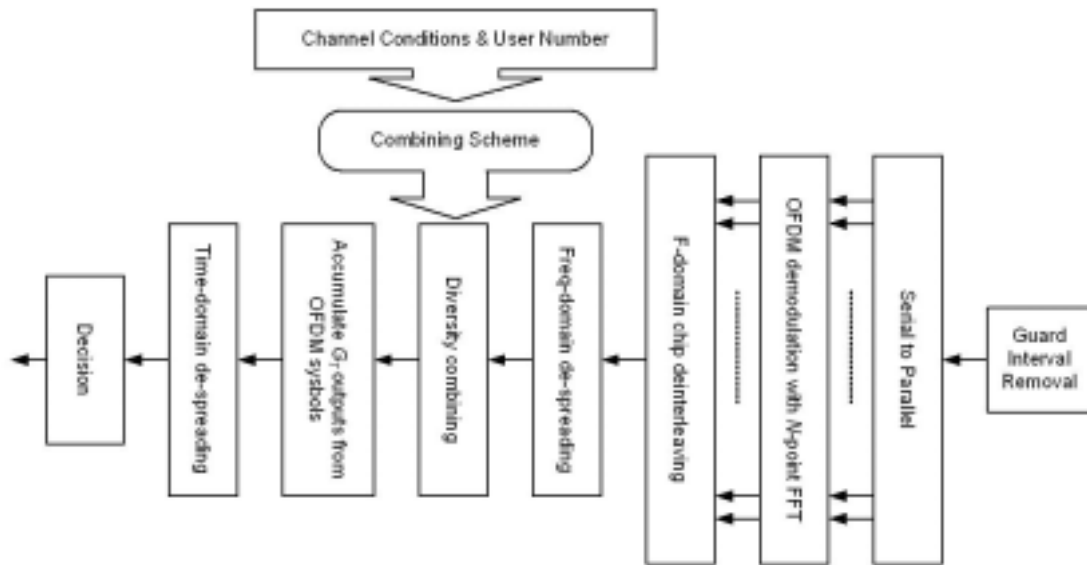


Fig. 2.13 The receiver structure of adaptive 2-D OFDM-CDMA systems

2.2.5 Simulation Configuration

Table 2.1 summarizes the major simulation parameters. We refer to the system parameters from the NTT DoCoMo papers [15].

Bandwidth	101.5MHz
Subcarrier frequency spacing	131.836 kHz
Number of subcarriers	768
IFFT/FFT points	1024
Spreading factor, SF	64
Spreading code	OVSF code
Symbol duration	1024(data)+226(guard)=1250 7.585+1.674=9.259 (usec)
Frequency and Time SF	2,4,8,16,32,64
Modulation scheme	QPSK

Table 2.1 Simulation parameters

The transmitted signals are subjected to broadband channel propagation as shown in Fig. 2.14. We assumed $L=6, 12, 24$ path Rayleigh fading channel with an exponential decay of the average received power levels with an interval of D_{exp} . The maximum delay and rms delay spread are shown in Table 2.2.

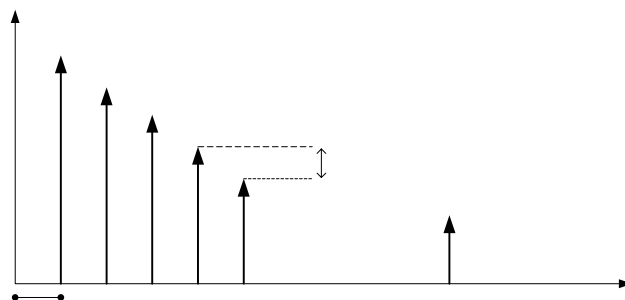


Fig. 2.14 Broadband channel model

L	Dexp (us)	Max. delay (us)	r.m.s delay spread (us)
6	0.0296(4 samples)	0.148(20 samples)	0.0424
12	0.0074(1sample)	0.0814(11 samples)	0.0215
12	0.0148(2 samples)	0.1628(22 samples)	0.0430
12	0.0296(4 samples)	0.3256(44 samples)	0.0860
12	0.0592(8 samples)	0.6512(88 samples)	0.1720
12	0.1184(16 samples)	1.3024(176 samples)	0.3440
24	0.0074(1 sample)	0.1702(23 samples)	0.0432

Table 2.2 Channel model parameters



Chapter 3

Adaptive Resource Allocation Methods

In the future, multimedia communications will be the main stream of wireless communication systems and realizing effective multi-rate physical-layer transmission becomes a highly challenging research in the current development of high speed wireless communications. Wideband and various data rate are the features of multimedia traffic. For multimedia traffic (voice, data, video) to be supported successfully, it is necessary to provide a QoS guarantee. QoS requirements can be specified by many different parameters: transmission rate, delay, or reliability being some of the most common. The radio resource management (RRM) entity is responsible for the correct use of the air interface resources in order to guarantee the quality to the offered services. Assume that the arrangement from RRM such as guaranteed data rate and total spreading factor is known, how to design an adaptive 2D OFDM-CDMA system in the physical layer to provide more flexible and efficient resource utilization is the most important issue in our research.

In Fig. 3.1, we illustrate a time-frequency resource plane which consists of many different color blocks with corresponding spreading factor. The square measure of one color block represents its corresponding total transmission data.

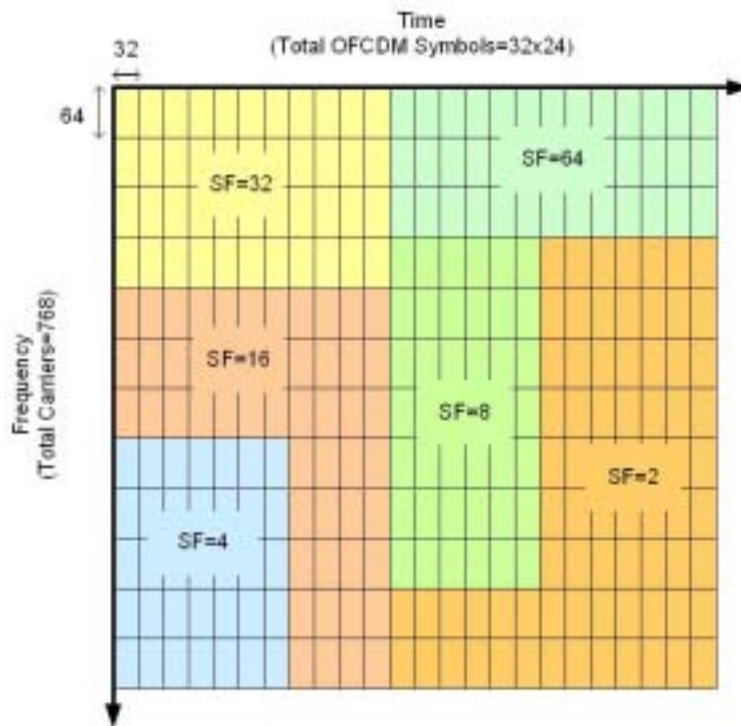


Fig. 3.1 The time-frequency resource plane in PHY layer

We find that the two main factors, frequency diversity and multiple access interference (MAI), dominate the system performance and there is a trade-off relation between the diversity gain and MAI. The radio link parameters and radio link conditions such like code-multiplexing user number, delay spread and Doppler frequency would cause frequency diversity, time diversity and MAI. The channel conditions and simultaneous user numbers can't be changed, but if we can design the system parameters to meet these conditions, the better BER performance would be achieved. Therefore, we would like to design some data allocation methods and use different combining schemes in order to get the most diversity gain and suppress MAI. We list four key points which affect the diversity gain and MAI.

- ◆ The length of spreading factor in the frequency domain and time domain
- ◆ Allocation methods for frequency sub-carriers and symbol time slots
- ◆ Code assignment of TF domain spreading codes for simultaneous users
- ◆ The diversity combining schemes employed in the receiver side

Some issues affect the frequency diversity and some influence MAI, but mostly the optimum design is achieved by jointly and adaptively considering all the issues. We explain the first three subjects respectively in this chapter and introduce the combining issues in Chapter 3 and Chapter 4.

3.1 Variable TF Spreading Factor Allocation

This sector involves two issues: one is the selection of time and frequency domain spreading factors, G_T and G_F , which determines the length of spreading factor, and the other is the allocation methods for OFDM time slots and frequency sub-carriers.

3.1.1 Selection of TF spreading factor

To provide more flexible and efficient resource utilization in physical layer, we partition the time-frequency resource plane into finer basic resource units. In Fig. 3.2, the square measure of each small block is 64-by-32, which means each block comprises 32 OFDM symbol time slots and each time slot has 64 sub-carriers. Then we partition the block into basic resource units according to its SF (G). G is a product

of T- and F-domain spreading code lengths, G_T and G_F , respectively. For example, the block whose SF equals 64 is partitioned into 32 32-by-2 basic units and the square measure of each basic unit is the same as its SF(G). And several typical spreading patterns are displayed in Fig.3-3, on which TF-domain spreading chips are mapped, so the block may be partitioned into 16-by-4 or 8-by-8 or 4-by-16 or 32-by-2 basic units. A G_T -by- G_F basic unit can support a maximum number of G simultaneous users with identical transmission rate, each of which is discriminated by a different orthogonal spreading code of length G .

We proceed to the optimum design of adaptive 2D OFDM-CDMA systems in the context of this 64-by-32 blocks. The design here is to optimize the BER performance over each block, by adaptively controlling some important system parameters.

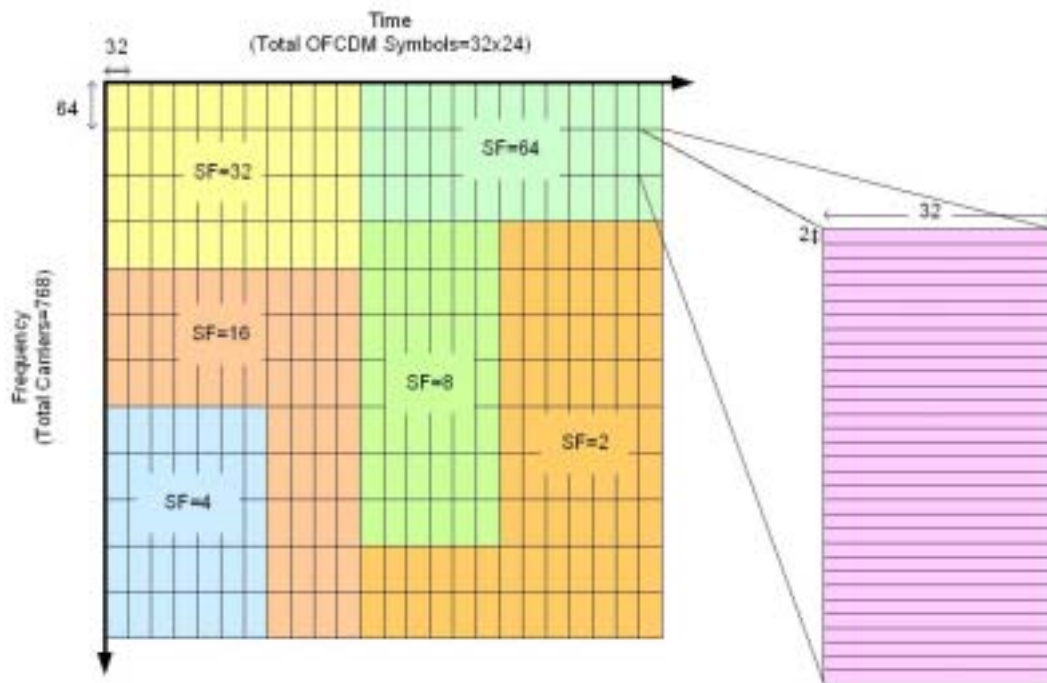


Fig. 3.2 The partition of time-frequency plane

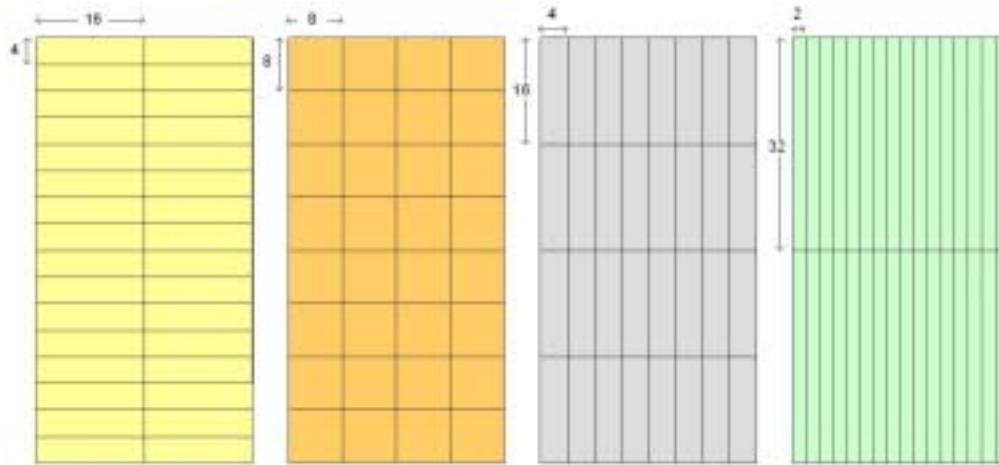


Fig. 3.3 Some typical spreading patterns

Although the square measures of basic units are all the same, different form of the basic units would bring out distinct MAI and diversity effect depending on the condition of propagation channels and the number of simultaneous users. We hope to get larger diversity gain and less MAI, however, they have trade off relationship. To get the diversity gain needs independent fading channel gains but to make MAI free needs the same fading channel gains. Observing the characteristic of the multi-path fading channels on OFDM systems, the time domain fading gains are transferred to frequency domain by FFT and each sub-carrier experiences different fading gain even if these sub-carriers are all in the coherent bandwidth. Therefore, spreading in the frequency domain would easily get the frequency diversity gain but it also easily causes MAI adverse effects. On the other hand, the variation of the fading gain in the time domain depends on the Doppler frequency. If the speed is low enough to ensure the time spreading period is in the coherent time, the fading gains would be all the same. As a result, MAI free appears in the time domain but on the contrary, there is no time diversity gain. In order to differentiate the effect between diversity and MAI, we use frequency domain spreading to get diversity and use successive time domain

spreading to sufficiently suppress MAI. Furthermore, the best balance between MAI and diversity and better BER performance could be achieved by adaptively controlling the size of time and frequency spreading factor.

3.1.2 Sub-carrier Allocation

In the last section we explain that the selection of allocation methods is a compromise between MAI and diversity. Diversity can significantly improve the average received signal power, but produce the orthogonality destruction for orthogonal spreading codes. We allocate sub-carriers separately in order to get frequency diversity. On the other hand, we allocate successive OFDM time slots for T- domain spreading, to effectively suppress MAI, at the cost of losing their respective diversity gains. Actually, the optimum selection of allocation methods for time/frequency sources closely depends on the condition of propagation channels and the number of simultaneous users.

In order to get the largest diversity gain, each sub-carrier need experience independent flat fading. We allocate interleaved sub-carriers in which the frequency separation between sub-carriers is maximized, to get the largest frequency diversity. Because of the interval between frequency spread period can't be infinity in reality, the fairer way is to average the interleaving distance in the total bandwidth.

Fig. 3.4 illustrates the interleaving allocation in the frequency domain. The interval between two sub-carriers depends on the size of G_F , the length of spreading factor in the frequency domain. The spreading sub-carriers are allocated in the equidistance (total carriers/ G_F). Therefore, if G_F is larger, the number of diversity

branches is also larger but may not get complete independent fading gain. On the contrary, less diversity branches but independent diversity gains are achieved if G_F is small.

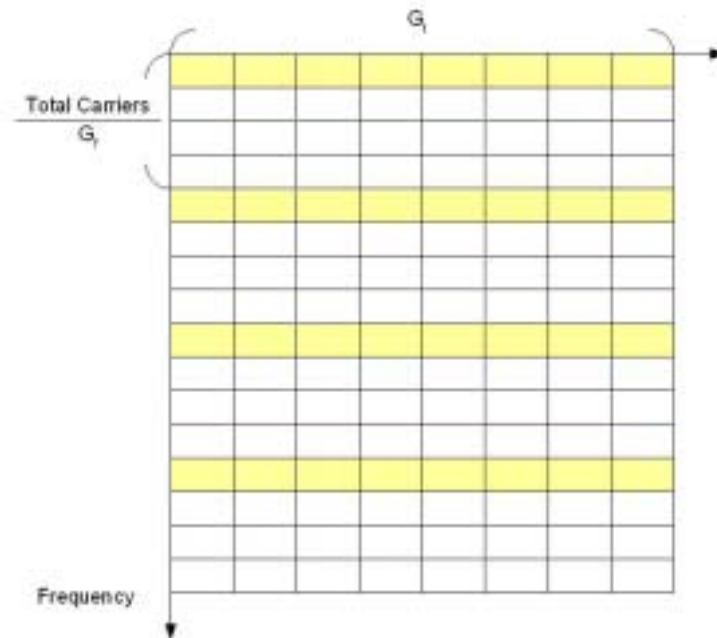


Fig. 3.4 Interleaving allocation in the frequency domain

Considering single user transmission, MAI problem could be dismissed. The BER performance of different spreading factor selection with channel delay spread $L=12$ is shown in Fig. 3.5. The best performance starts from the curve of $G_F=16$, and the curves with G_F larger than 16 have the same performance. This is because there is enough independent fading to make frequency diversity saturated. And the interval with $G_F=16$ between two spreading sub-carriers is approximately equal to the coherent bandwidth of the channel. So we can choose the spreading factor G_F and G_T based on the coherent bandwidth. Fig. 3.6 shows BER curves of delay spread $L=6$. The curves of $G_F \geq 8$ have the best performance. We can arbitrarily choose any one spreading pattern whose diversity is enough when single user transmission. But if many user transmit simultaneously, we need to adaptively choose the (G_T, G_F)

according to the user number and the combining methods. The problem is more complex because multi-user transmission would bring about MAI, and total issues should be jointly considered. We will discuss these issues in next section.

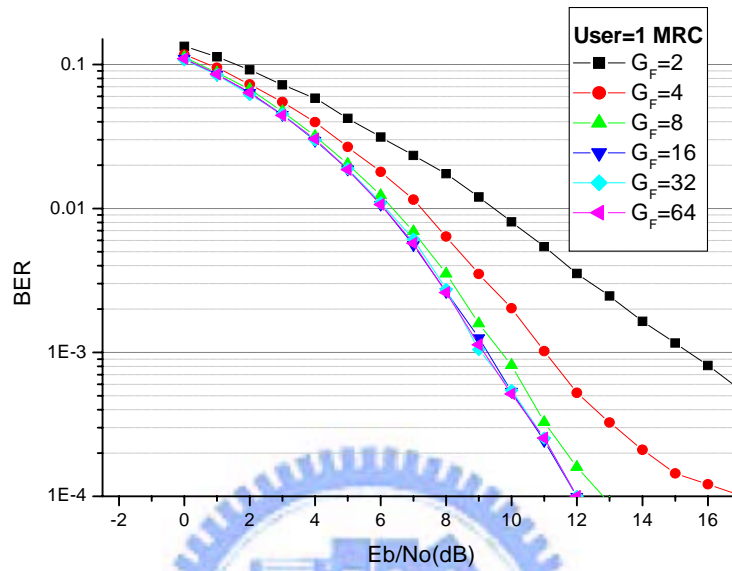


Fig. 3.5 Performance comparisons between different spreading patterns for single user case with MRC detection and delay spread $L=12$

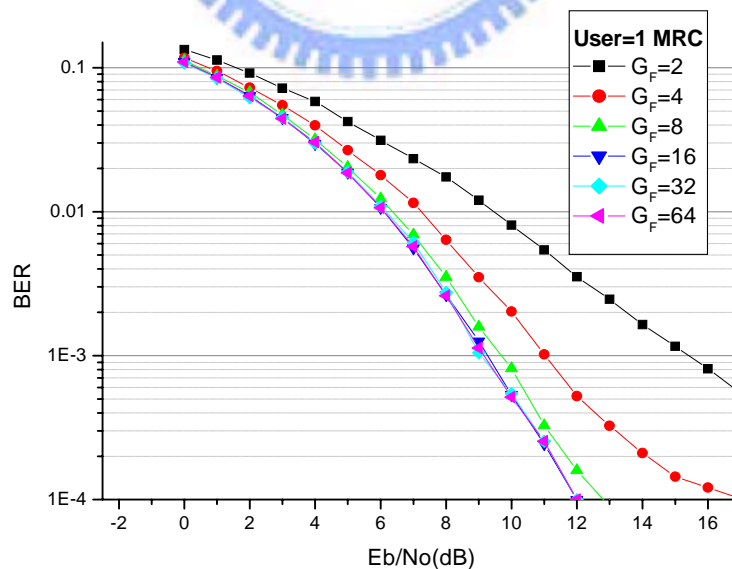


Fig. 3.6 Performance comparisons between different spreading patterns for single user case with MRC detection and delay spread $L=6$

3.2 Spreading Code Assignment

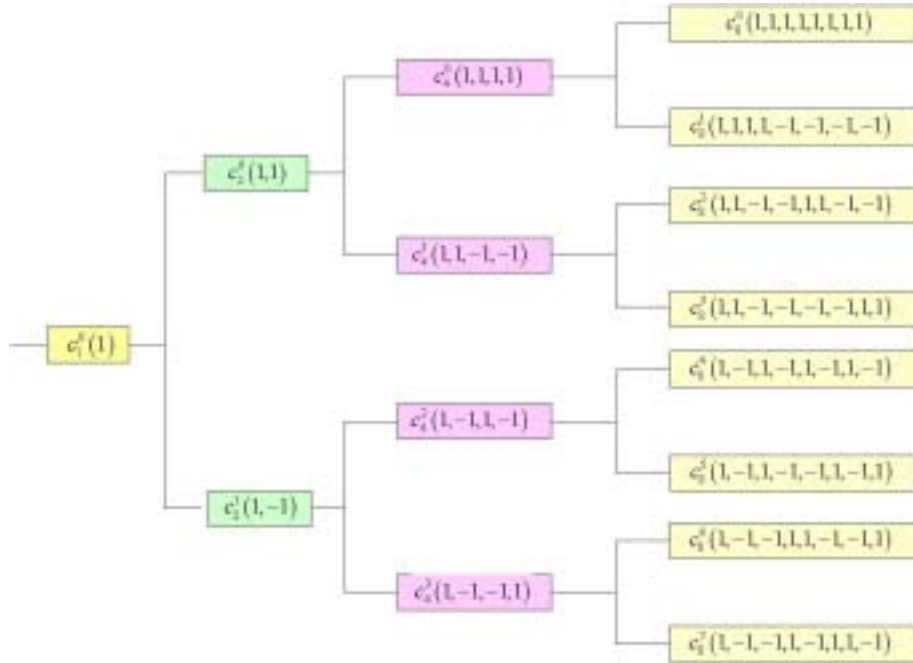


Fig. 3.7 OVSF code tree

We have introduced the principle of Orthogonal Variable Spreading Factor (OVSF) code in Chapter 2 and Fig. 3.7 shows the code tree of OVSF code. Any two OVSF codes are orthogonal to each other originally but after experiencing the multi-path channel, the code orthogonality may be destroyed and cause MAI effect. According to the channel condition, a set of spreading code is decided to get the largest frequency diversity gain. When the user number increases, how to select the code sets to avoid MAI effect becomes the important issue. Observing the spreading codes in Fig. 3.7, the SF (G) is eight to provide 8 codes from C_8^0 to C_8^7 . If we choose $(G_T, G_F)=(4,2)$ to satisfy $G = G_F G_T$, it represents the data is spread over four OFDM time slots which have two sub-carriers respectively. Because of the characteristic of OVSF code, each code (C_8) is the product of its two root codes (C_2 and C_4) in the

Fig. 3.8. Each user can choose a combination of C_2 and C_4 code to represent the frequency and time domain spreading code respectively.

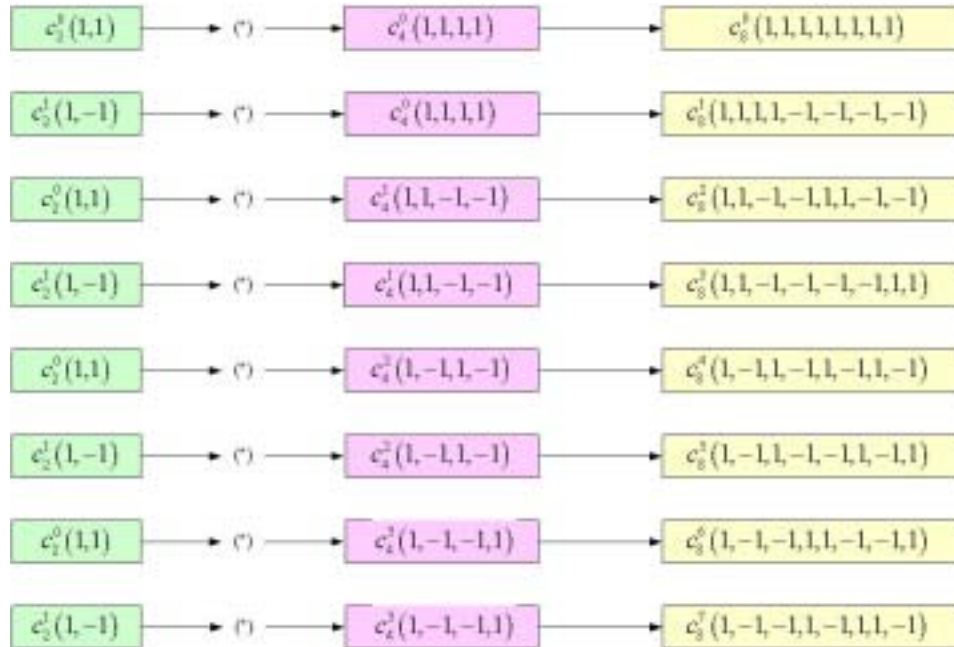


Fig. 3.8 The pairs of time and frequency spreading codes

Any code can be chosen when there is only one transmitter user but the code assignment issue should be considered when the user number is greater than one. This is because that the channel effect would not destruct the code orthogonality if we choose right pairs of the codes.

For example, Fig. 3.9 shows that the code sets $(G_T, G_F)=(4,2)$ are used on the left figure. After the time spreading code multiplying frequency spreading code, the code length is eight and the code arranges in order in the figure on the right. At transmitter side, they are orthogonal to each other. Assume the time spread period is smaller than the coherent time so the channel gains are all the same but the data

experience independent fading gains in the frequency domain. Fig. 3.10 displays the result of transmit data multiplying the channel gain. The 1st code and the 2nd code still maintain orthogonality but the 1st code and the 5th code lose the orthogonality and cause severe MAI. This is because the time spread codes of the 1st and the 2nd code are different, and even the channel gains in the frequency domain are different, it would not bring out MAI problem.

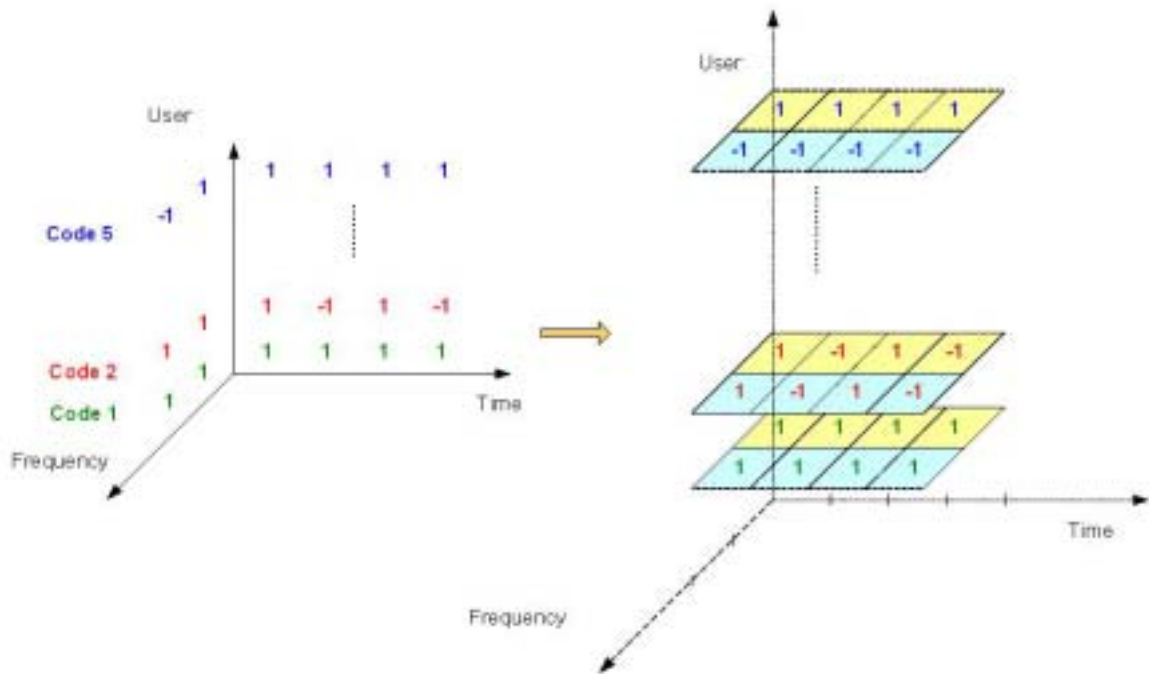


Fig. 3.9 Time and frequency code assignment

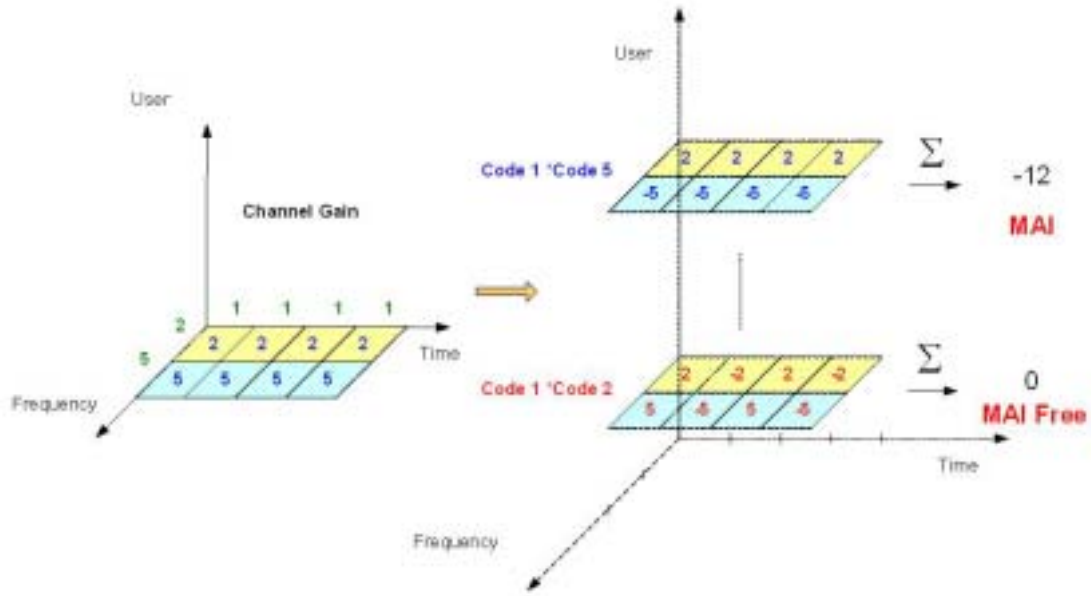


Fig. 3.10 The relation between code assignment and MAI

From example, we know that using the same time spreading codes would cause severe MAI. Therefore, if there are more than two simultaneous users, “different time spreading codes” have the priority in the code assignment issues. Then the other points in the code assignment issues are how many codes can be used and what is their priority? It is found that the number G of spreading codes can be separated into G_F number of codesets and each codeset has number G_T time domain spreading codes as shown in the Fig.3.11. Therefore, when user number is less than G_T , we can choose the spreading factor in order in the first codeset. Each codeset has the same frequency domain spreading code and different time domain spreading codes. When user number is larger than G_T , we choose the spreading factors in order at the codeset 2, codeset 3, ..., and so on.

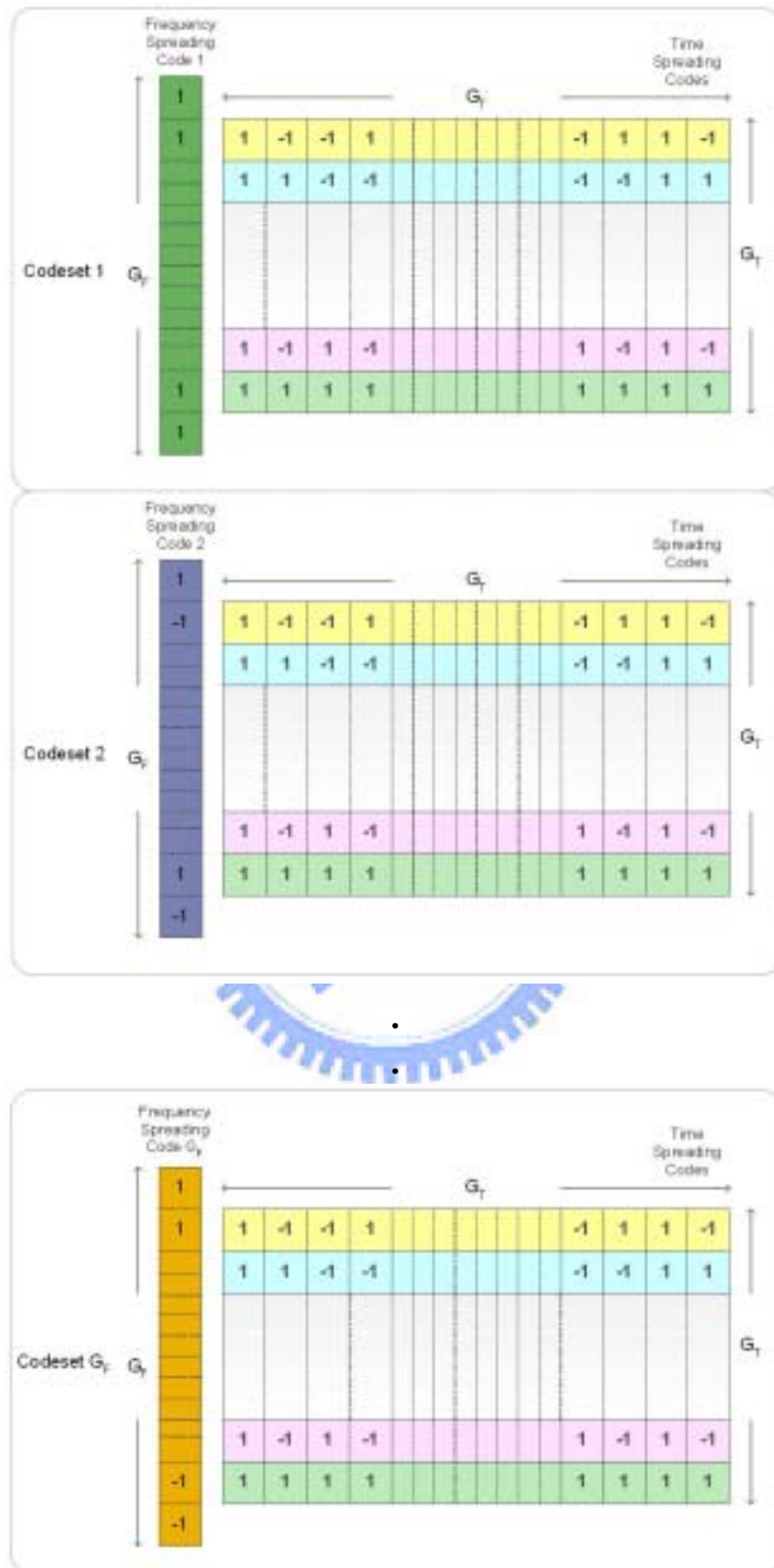


Fig. 3.11 The priority of code assignment

Fig 3.12 shows the BER performance with better code assignment. From user number from 1 to 32, the MAI is free if the code assignment is performed. On the contrary, Fig. 3.13 shows the performance with worse code assignment. When the second user is allocated the same time spreading code with the first user, the BER performance degrades severely due to large MAI effect.

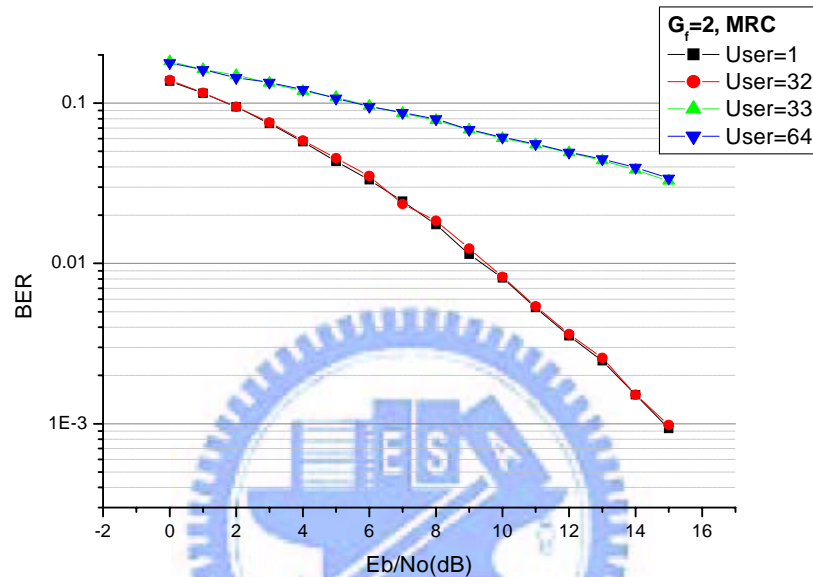


Fig. 3.12 Performance of better code assignment with different user number

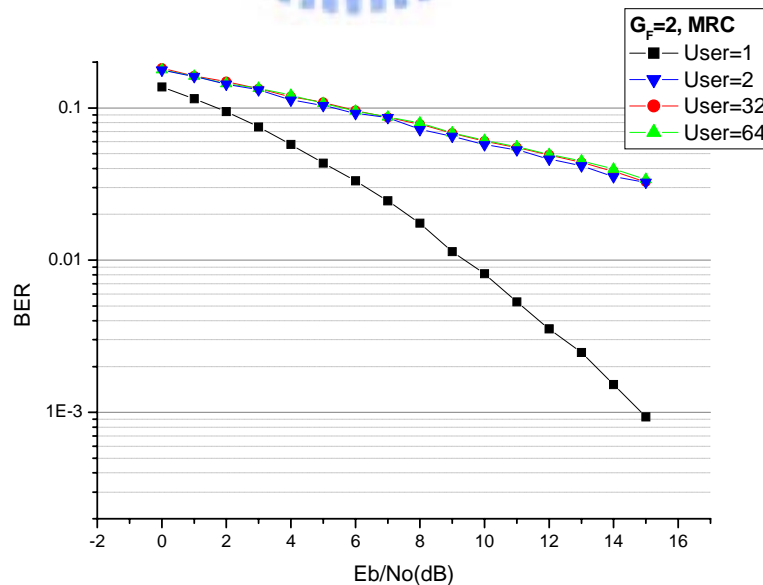


Fig. 3.13 Performance of worse code assignment with different user number

Fig. 3.14 shows the MAI between desired user 1 and other users. When the spreading pattern $(G_T, G_F) = (32, 2)$, user 33 is the only one interference user but the interference power is very large. On the contrary, when the user number $(G_T, G_F) = (1, 64)$, any other user would bring interference but the MAI power is very small.

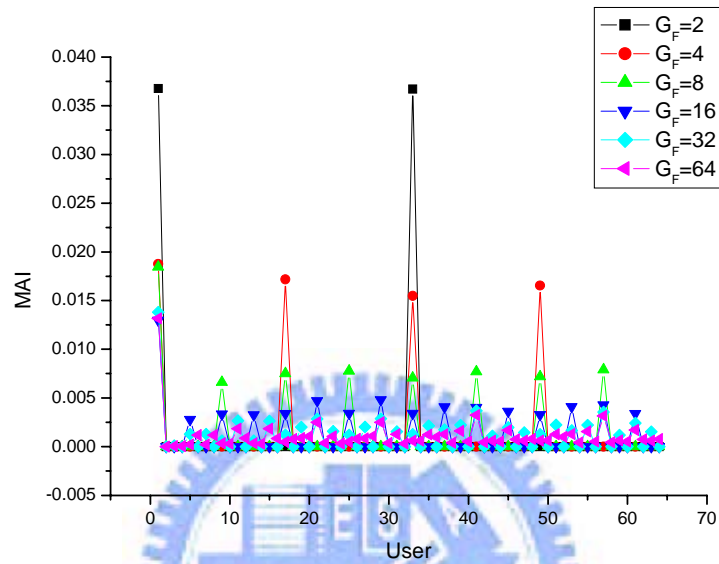


Fig. 3.14 MAI power between desired user and other users

Chapter 4

Single User Detection

Following the last section, we will continue introducing the receiver combining issues and how to joint design in the adaptive 2D OFDM-CDMA systems. First we discuss single user detection schemes. Diversity combining schemes are used to minimize noise, suppress MAI, optimize diversity benefits, or perform some combinations of them. An adaptive 2D OFDM-CDMA system could change its spreading pattern according to different channels conditions. Some spreading patterns might retain the orthogonality among simultaneous users employed the same BRU. The others, however, might inevitably suffer the MAI. Consequently, it is necessary to select an appropriate combining scheme at receiver in accordance with the condition of propagation channel and spreading pattern. Specifically, the most commonly used combining schemes include [3]: MRC (Maximum Ratio Combining), EGC (Equal Gain Combining), ORC (Orthogonality Restoring Combining), and MMSEC (Minimized Mean Square Error Combining).

4.1 Maximum Ratio Combining (MRC)

In the single-user case (MAI free), MRC is the optimal diversity combining scheme in the sense of maximizing the combining output SNR. With MRC, the

diversity branches are weighted by their respective complex fading gains and then combined. For this detector,

$$G_k = H_k^* \quad (4.1)$$

In the multi-user case, the MRC detector will not give optimal performance here. This is because MRC only considers the noise effect and does not consider the orthogonality property. The decision variable after combining is,

$$\begin{aligned}
D_p^1 = & \underbrace{d_p^1 \sum_{i=1}^{G_F} \sum_{j=1}^{G_T} |H_{i+p \cdot G_F, j}| \cdot |H_{i+p \cdot G_F, j}|^*}_{\text{desired signal}} \\
& + \underbrace{\sum_{u=2}^{N_u} \sum_{i=1}^{G_F} \sum_{j=1}^{G_T} d_p^u |H_{i+p \cdot G_F, j}| \cdot |H_{i+p \cdot G_F, j}|^* \cdot cf_i^1 \cdot ct_j^1 \cdot cf_i^u \cdot ct_j^u}_{\text{MAI}} \\
& + \underbrace{\sum_{i=1}^{G_F} \sum_{j=1}^{G_T} z_{i+p \cdot G_F, j} \cdot |H_{i+p \cdot G_F, j}|^* \cdot cf_i^1 \cdot ct_j^1}_{\text{noise}}
\end{aligned} \quad (4.2)$$

Observing the MAI item, when the user number increases, MAI becomes a multiple proportion to the square of fading channel gains. As a result, it degrades the system performance severely.

From Fig.4.1 to Fig.4.5, we compare the BER performances of different pairs of time and frequency domain spreading factors with MRC detection and user number equals 1,4,8,16,32, respectively. The diversity issue based on SF size allocation has been discussed in Section II. We know that the diversity gain is saturated from frequency spreading factor $G_F=16$, so the spreading patterns of $G_F=32, 64$ also have the same performance in single user case in Fig. 4.1. When user number equals 4 in Fig. 4.2, the spreading patterns using $G_F=2, 4, 8, 16$ and code assignment mentioned before are MAI free. Although using spreading codes which $G_F=32, 64$

already have MAI, the interference effect is too little to degrade BER performance. But when user number adds to 8 in Fig. 4.3, the curve $G_F=16$ is not the best because it corresponds to $G_T=4$. According to code assignment, the simultaneous users would use the same time domain spreading codes if user number is larger than 4. The MAI is large enough to degrade BER performance so now $G_F=8$ is the best choice. For the same reason, we find the best BER performance in Fig.4.4 is frequency spreading code of $G_F=4$ corresponding to user number equals 16, and the code of $G_F=2$ corresponding to 32 users in Fig.4.5.

In conclusion, MRC is a good method in single-user or MAI free condition, but it has poor ability to suppress MAI. When MAI occurs, diversity is not the decisive factor because MAI would dominate the performance.

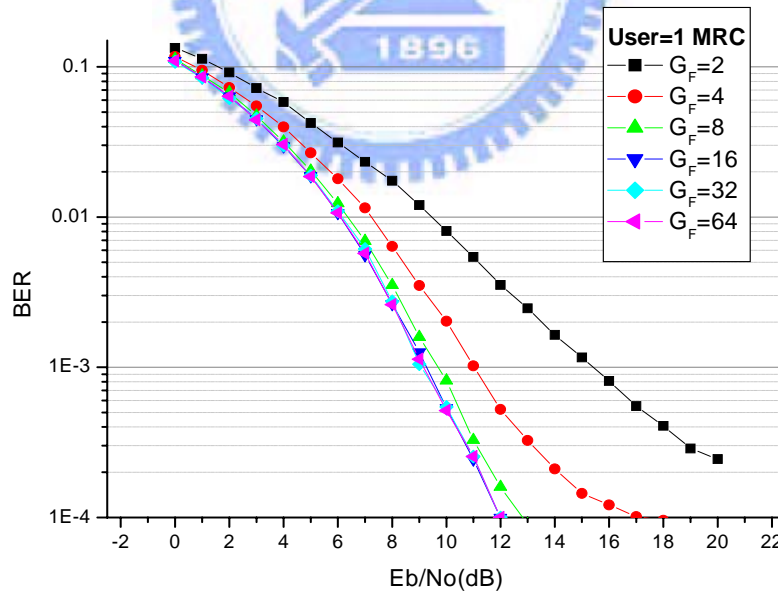


Fig. 4.1 Performance comparisons of different spreading patterns with user number=1 and MRC detection

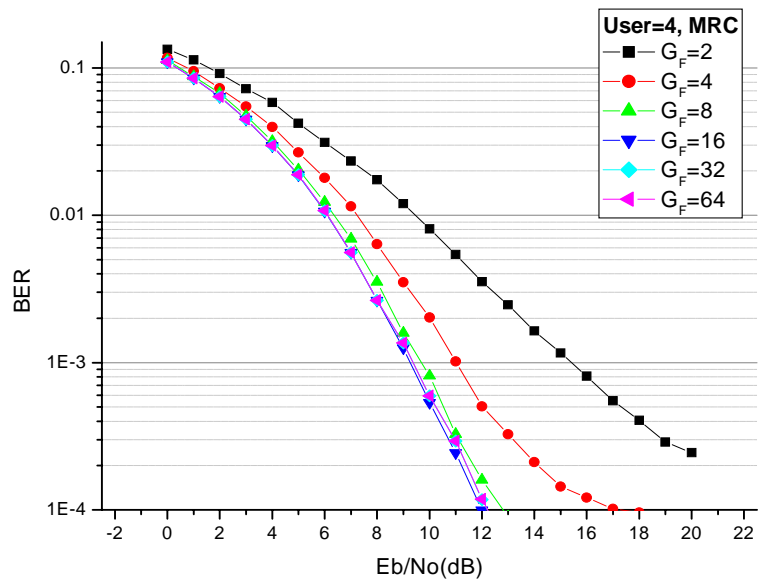


Fig. 4.2 Performance comparisons of different spreading patterns with user number= 4 and MRC detection

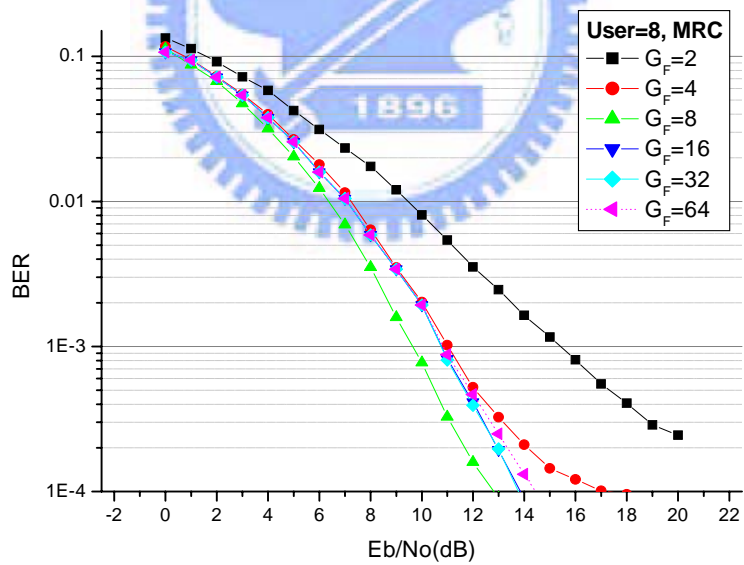


Fig. 4.3 Performance comparisons of different spreading patterns with user number=8 and MRC detection

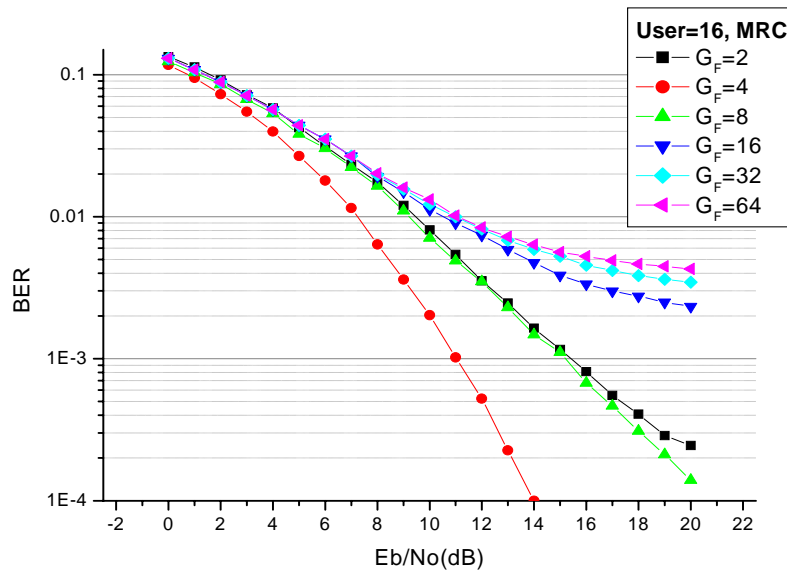


Fig. 4.4 Performance comparisons of different spreading patterns with user number=16 and MRC detection

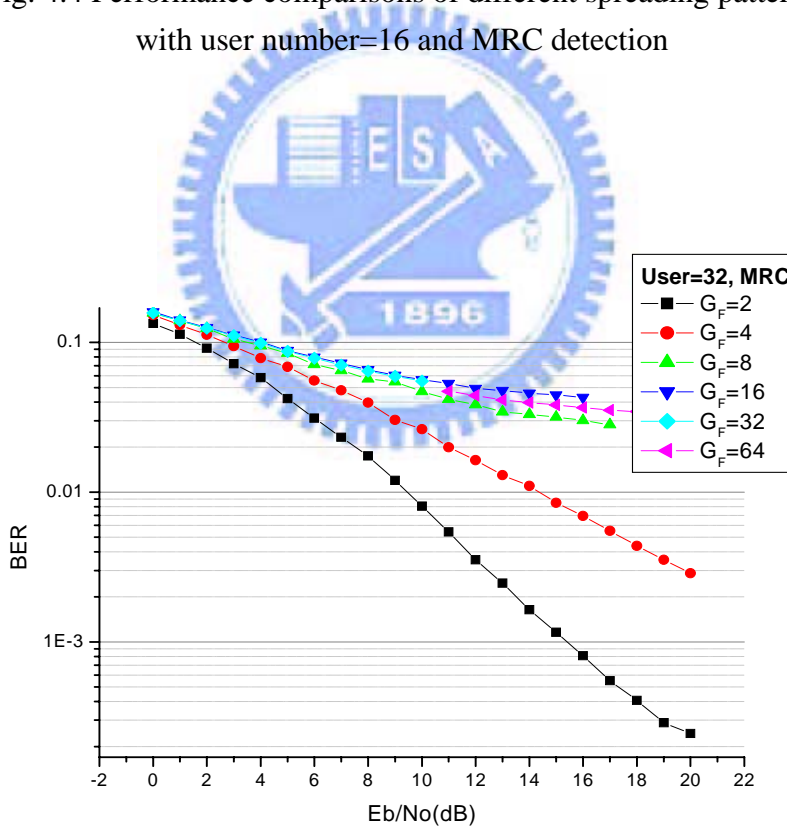


Fig. 4.5 Performance comparisons of different spreading patterns with user number=32 and MRC detection

4.2 Equal Gain Combining (EGC)

EGC is similar to MRC because of the co-phased combining, but different from MRC because the diversity branches are not weighted. In certain cases, it is not convenient to provide for the variable fading gains required for MRC, and EGC will be a practical selection instead of MRC. Similarly, the selectivity of the radio channel produces the orthogonality destruction but not worse than MRC.

The simplest detector is EGC and the combining weight is,

$$G_k = \frac{H_k^*}{|H_k|} \quad (4.3)$$

As we can see, EGC can only correct the phase shift at each sub-carrier. After combining, the decision variable is

$$\begin{aligned}
 D_p^1 = & \underbrace{d_p^1 \sum_{i=1}^{G_F} \sum_{j=1}^{G_T} |H_{i+p \cdot G_F, j}| \cdot \frac{H_{i+p \cdot G_F, j}^*}{|H_{i+p \cdot G_F, j}|}}_{\text{desired signal}} \\
 & + \underbrace{\sum_{u=2}^{N_u} \sum_{i=1}^{G_F} \sum_{j=1}^{G_T} d_p^u |H_{i+p \cdot G_F, j}| \cdot \frac{H_{i+p \cdot G_F, j}^*}{|H_{i+p \cdot G_F, j}|} \cdot cf_i^1 \cdot ct_j^1 \cdot cf_i^u \cdot ct_j^u}_{MAI} \\
 & + \underbrace{\sum_{i=1}^{G_F} \sum_{j=1}^{G_T} z_{i+p \cdot G_F, j} \cdot \frac{H_{i+p \cdot G_F, j}^*}{|H_{i+p \cdot G_F, j}|} \cdot cf_i^1 \cdot ct_j^1}_{\text{noise}}
 \end{aligned} \quad (4.4)$$

Comparing with MRC, the BER performance of EGC is worse than MRC in single-user condition, because EGC doesn't maximize SNR. On the contrary, EGC has better performance in multi-user case because it just multiples the magnitude of

fading gains and wouldn't amplify MAI as much as MRC. In Fig. 4.6, the BER performance demonstrates the inference.

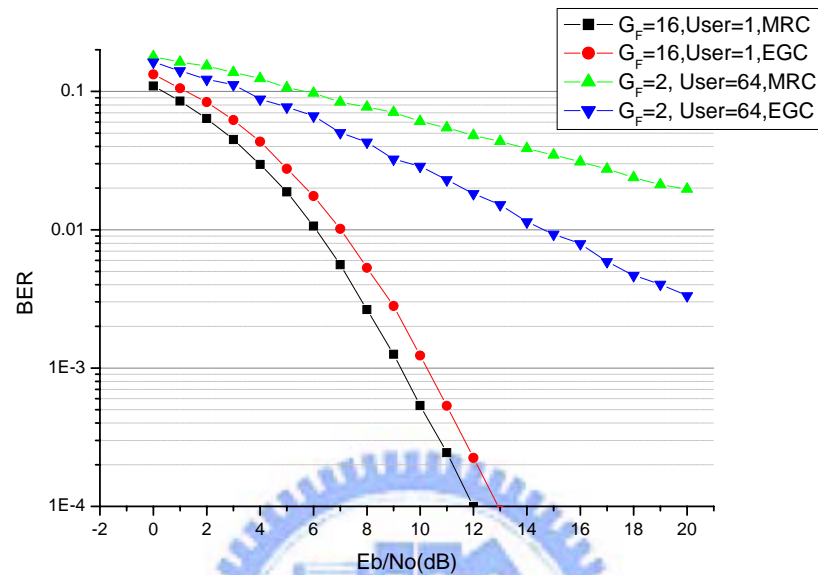


Fig.4.6 Performance comparisons of different spreading patterns with EGC detection

For the downlink transmission, if the phase distortion for each sub-carrier is perfectly corrected, the gain for EGC is just a constant. This is a very simple detector and useful in real implementation.

4.3 Orthogonality Restoring Combining (ORC)

ORC performs well in the case of MAI by restoring orthogonality between codes. The ORC equalizes each diversity branch using the combining weight in inverse proportion to the corresponding channel gain. It can perfectly restore orthogonality but produces noise enhancement. The ORC detector compensates for the channel effect completely. The gain for each sub-carrier is,

$$G_k = \frac{H_k^*}{|H_k|^2} \quad (4.5)$$

Since the channel effect is completely removed, the code orthogonality is preserved. However, noise may be greatly amplified for sub-carriers with low SNR. The combining result is then

$$\begin{aligned}
 D_p^1 &= \underbrace{d_p^1 \sum_{i=1}^{G_F} \sum_{j=1}^{G_T} |H_{i+p \cdot G_F, j}| \cdot \frac{H_{i+p \cdot G_F, j}^*}{|H_{i+p \cdot G_F, j}|^2}}_{\text{desired signal}} \\
 &+ \underbrace{\sum_{u=2}^{N_u} \sum_{i=1}^{G_F} \sum_{j=1}^{G_T} d_p^u |H_{i+p \cdot G_F, j}| \cdot \frac{H_{i+p \cdot G_F, j}^*}{|H_{i+p \cdot G_F, j}|^2} \cdot cf_i^1 \cdot ct_j^1 \cdot cf_i^u \cdot ct_j^u}_{\text{MAI}} \\
 &+ \underbrace{\sum_{i=1}^{G_F} \sum_{j=1}^{G_T} z_{i+p \cdot G_F, j} \cdot \frac{H_{i+p \cdot G_F, j}^*}{|H_{i+p \cdot G_F, j}|^2} \cdot cf_i^1 \cdot ct_j^1}_{\text{noise}}
 \end{aligned} \quad (4.6)$$

If transmission is downlink, we can get the modified MAI

$$\underbrace{\sum_{u=2}^{N_u} \sum_{i=1}^{G_F} \sum_{j=1}^{G_T} d_p^u \cdot cf_i^1 \cdot ct_j^1 \cdot cf_i^u \cdot ct_j^u}_{\text{MAI}} = 0 \quad (4.7)$$

But the noise enhancement degrades the performance severely.

4.4 Minimum Mean Square Error Combining (MMSEC)

The MMSE detector is obtained by minimizing the mean square errors between the detected data and the original data. The MMSE detector can be divided into two methods, MMSE per user detector and MMSE per carrier detector.

MMSE per carrier detector

The MMSE per carrier detector attempts to invert each sub-channel coefficient, applying the MMSE criterion in order to avoid excessive noise enhancement.

In the receiver side, we obtain

$$\begin{aligned}
 r_{i,j} &= \sum_{u=1}^{N_b} d^u \cdot c f_i^u \cdot c t_j^u \cdot H_{i,j} + n_{i,j} \\
 &= D_{i,j} \cdot H_{i,j} + n_{i,j}
 \end{aligned} \tag{4.8}$$

where $D_{i,j} = \sum_{u=1}^{N_b} d^u \cdot c f_i^u \cdot c t_j^u$

The optimization criterion is to find for each sub-channel a filter coefficient that multiplies the observation given in such that (We can omit the subscription p without loss of generality.)

$$W_{i,j} = \arg \min_{W_{i,j}} E \left\{ \left| D_{i,j} - W_{i,j} \cdot r_{i,j} \right|^2 \right\} \tag{4.9}$$

The solution is obtained by applying the Wiener Solution

$$W_{i,j} = \mathbf{R}_{Dr} \cdot \mathbf{R}_{rr}^{-1} \tag{4.10}$$

The $\mathbf{R}_{\mathbf{Dr}}$ is obtained as

$$\begin{aligned}
\mathbf{R}_{\mathbf{Dr}} &= E\{D_{i,j} \cdot r_{i,j}^*\} = E\left\{D_{i,j} \cdot \left(\sum_{u=1}^{N_u} d^u \cdot cf_i^u \cdot ct_j^u \cdot H_{i,j} + n_{i,j}\right)^*\right\} \\
&= E\left\{\left(\sum_{u=1}^{N_u} d^u \cdot cf_i^u \cdot ct_j^u\right) \cdot \left(\sum_{u=1}^{N_u} d^u \cdot cf_i^u \cdot ct_j^u \cdot H_{i,j} + n_{i,j}\right)^*\right\} \\
&= E\left\{\left(\sum_{u=1}^{N_u} d^u \cdot cf_i^u \cdot ct_j^u\right) \cdot \left(\sum_{u=1}^{N_u} d^u \cdot cf_i^u \cdot ct_j^u \cdot H_{i,j}\right)^*\right\} + E\left\{\left(\sum_{u=1}^{N_u} d^u \cdot cf_i^u \cdot ct_j^u\right) \cdot n_{i,j}^*\right\} \\
&= H_{i,j}^* \cdot E\left\{\left(\sum_{u=1}^{N_u} d^u \cdot cf_i^u \cdot ct_j^u\right) \cdot \left(\sum_{u=1}^{N_u} (d^u)^* \cdot cf_i^u \cdot ct_j^u\right)\right\} \\
&= H_{i,j}^* \cdot N_u \\
&\text{assume } E\left\{\left(d^p \cdot cf_i^p \cdot ct_j^p\right) \cdot \left((d^q)^* \cdot cf_i^q \cdot ct_j^q\right)\right\} = \begin{cases} 0, & \text{if } p \neq q \\ 1, & \text{if } p = q \end{cases} \\
&E\left\{\left(\sum_{u=1}^{N_u} d^u \cdot cf_i^u \cdot ct_j^u\right) \cdot n_{i,j}^*\right\} = 0
\end{aligned} \tag{4.11}$$

The $\mathbf{R}_{\mathbf{rr}}$ is obtained as

$$\begin{aligned}
\mathbf{R}_{\mathbf{rr}} &= E\{r_{i,j} \cdot r_{i,j}^*\} = E\left\{\left(\sum_{u=1}^{N_u} d^u \cdot cf_i^u \cdot ct_j^u \cdot H_{i,j} + n_{i,j}\right) \cdot \left(\sum_{u=1}^{N_u} d^u \cdot cf_i^u \cdot ct_j^u \cdot H_{i,j} + n_{i,j}\right)^*\right\} \\
&= |H_{i,j}|^2 \cdot E\left\{\left(\sum_{u=1}^{N_u} d^u \cdot cf_i^u \cdot ct_j^u\right) \cdot \left(\sum_{u=1}^{N_u} d^u \cdot cf_i^u \cdot ct_j^u\right)^*\right\} + E\left\{\left(\sum_{u=1}^{N_u} d^u \cdot cf_i^u \cdot ct_j^u\right) \cdot n_{i,j}^*\right\} \\
&+ E\left\{\left(\sum_{u=1}^{N_u} d^u \cdot cf_i^u \cdot ct_j^u\right)^* \cdot n_{i,j}\right\} + E\{n_{i,j} \cdot n_{i,j}^*\} \\
&= |H_{i,j}|^2 \cdot N_u + \sigma_n^2 \\
&\text{where } E\left\{\left(\sum_{u=1}^{N_u} d^u \cdot cf_i^u \cdot ct_j^u\right) \cdot n_{i,j}^*\right\} = 0 \\
&E\{n_{i,j} \cdot n_{i,j}^*\} = \sigma_n^2
\end{aligned} \tag{4.12}$$

So we get the combining weight

$$\begin{aligned}
W_{i,j} &= \mathbf{R}_{Dr} \cdot \mathbf{R}_{rr}^{-1} \\
&= \frac{P_c \cdot H_{i,j}^* \cdot N_u}{P_c \cdot |H_{i,j}|^2 \cdot N_u + \sigma_n^2} \\
&= \frac{H_{i,j}^*}{|H_{i,j}|^2 + \frac{\sigma_n^2}{N_u \cdot P_c}}
\end{aligned} \tag{4.13}$$

Then the decision variable is

$$\begin{aligned}
D_p^1 &= \underbrace{d_p^1 \sum_{i=1}^{G_F} \sum_{j=1}^{G_T} |H_{i+p \cdot G_F, j}| \cdot \frac{H_{i+p \cdot G_F, j}^*}{|H_{i+p \cdot G_F, j}|^2 + \frac{\sigma_n^2}{J\sigma_s^2}}}_{\text{desired signal}} \\
&+ \underbrace{\sum_{u=2}^{N_u} \sum_{i=1}^{G_F} \sum_{j=1}^{G_T} d_p^u |H_{i+p \cdot G_F, j}| \cdot \frac{H_{i+p \cdot G_F, j}^*}{|H_{i+p \cdot G_F, j}|^2 + \frac{\sigma_n^2}{J\sigma_s^2}} \cdot cf_i^1 \cdot ct_j^1 \cdot cf_i^u \cdot ct_j^u}_{\text{MAI}} \\
&+ \underbrace{\sum_{i=1}^{G_F} \sum_{j=1}^{G_T} z_{i+p \cdot G_F, j} \cdot \frac{H_{i+p \cdot G_F, j}^*}{|H_{i+p \cdot G_F, j}|^2 + \frac{\sigma_n^2}{J\sigma_s^2}} \cdot cf_i^1 \cdot ct_j^1}_{\text{noise}}
\end{aligned} \tag{4.14}$$

Unlike MRC, EGC, ORC detectors, MMSE detector makes a compromise between noise enhancement and MAI to get better performance. However, it requires additional side information. From (4.13), the number of user and noise power must be known. The number of user should be notified to mobile and the noise power must be estimated.

Fig. 4.7 shows the single-user performance. As the result mentioned before, $G_F=16, 32, 64$ have largest diversity gains. And we find that the $G_F=16$ has the best BER performance from light load to heavy load. In Fig. 4.8, the $G_F=16$ is better than

$G_F = 64$ (MC-CDMA) with 3 dB gain. This is because not only no additional diversity gain with $G_F = 64$ but increase the MAI. Therefore, MMSE is different from MRC and EGC by choosing spreading patterns based on channel coherent bandwidth but not user number and it ascribes to better ability to suppress MAI.

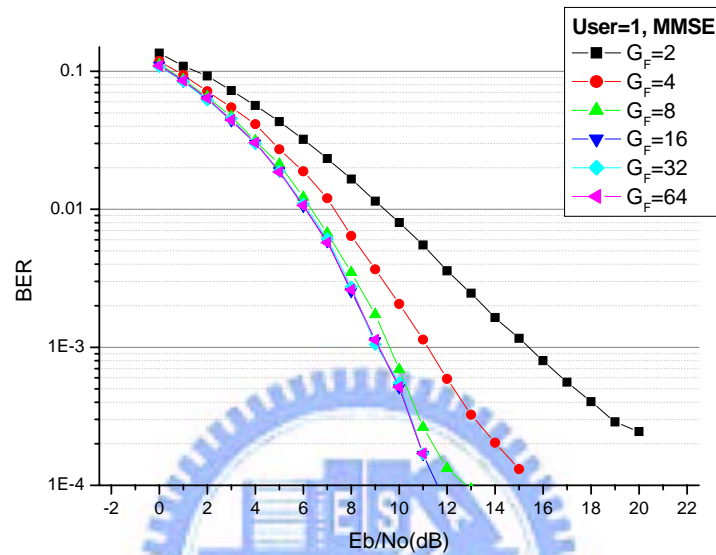


Fig. 4.7 Performance comparisons of different spreading patterns with user number = 1 and MMSE detector

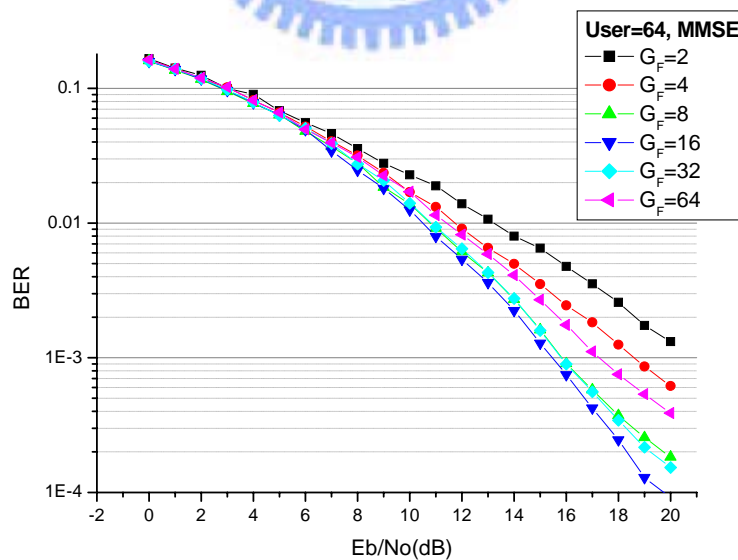


Fig. 4.8 Performance comparisons of different spreading patterns with user number = 64 and MMSE detector

4.5 Composite Discussion of Single User Detection

The performance comparisons between three single user detection methods with different user number are shown below. Fig.4.9 shows the performance of single user and Fig.4.10 shows the performance of user number equals 4. Because there is no interference when user number equals 4 with $G_F = 16$, the performance of user number = 4 is equal to single user. The MRC detector has the best BER performance.

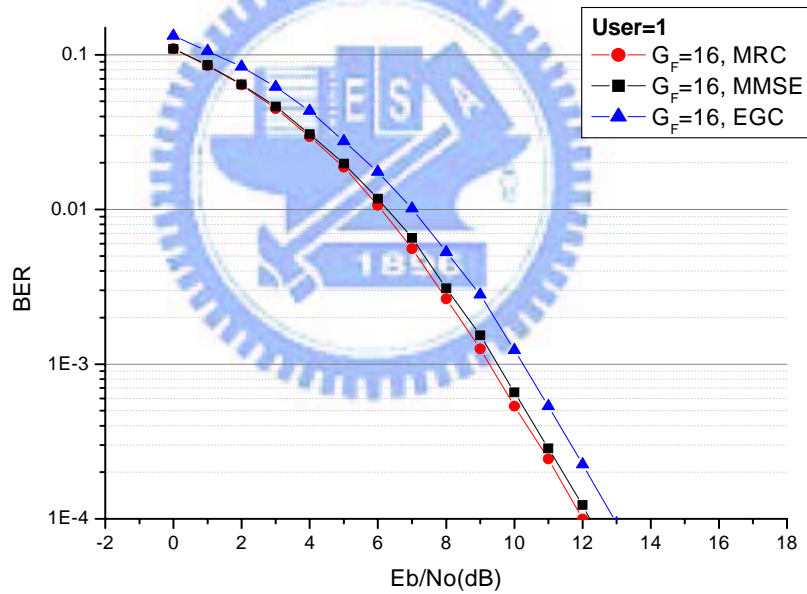


Fig.4.9 Performance comparison between single user detection with user number =1

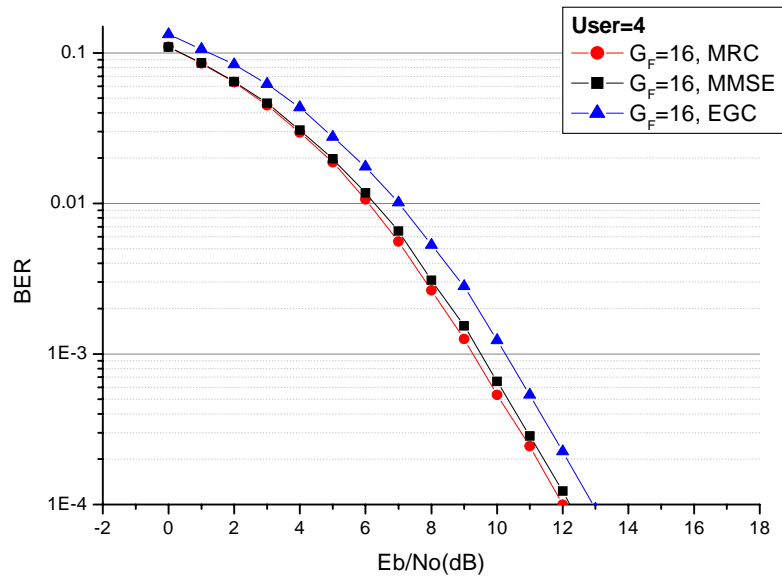


Fig.4.10 Performance comparison between single user detection with user number =4

When user number equals 8 in Fig.4.11, MRC and EGC detectors with spreading patterns of $G_F = 8$ maintain MAI free and MMSE with spreading pattern $G_F = 16$ has the largest diversity gain. The result shows the MRC still has the best performance between three methods. And the similar results appear in the Fig.4.11 and Fig.4.12. MRC is the best detector while maintaining MAI free.

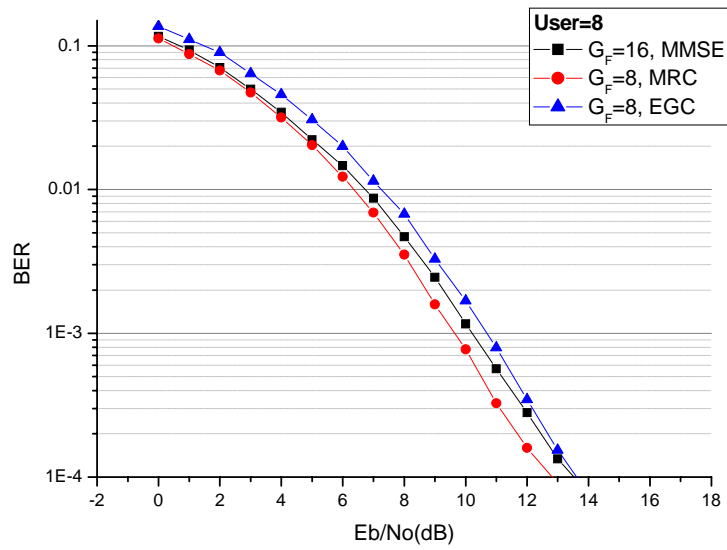


Fig.4.11 Performance comparison between single user detection with user number = 8

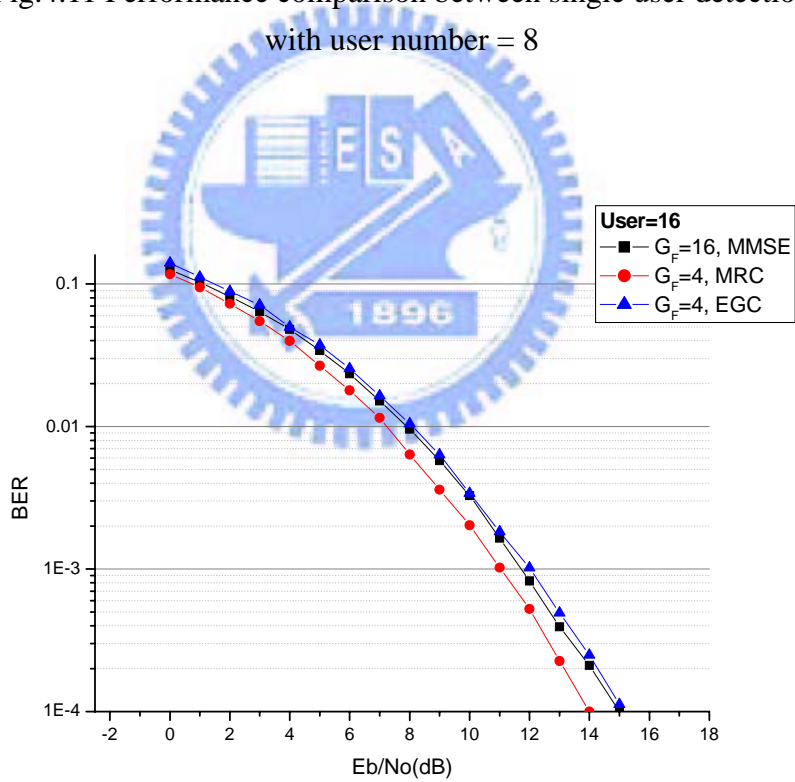


Fig.4.12 Performance comparison between single user detection with user number = 16

When user number increases to 32 in Fig.4.13, MMSE displays its great ability to suppress MAI. Although MRC still maintain orthogonality but it is not the best detector due to insufficient diversity gain. And MAI degrades the MRC performance severely for user number = 64 case in Fig.4.14. Therefore, we should choose MMSE detector for heavy load conditions.

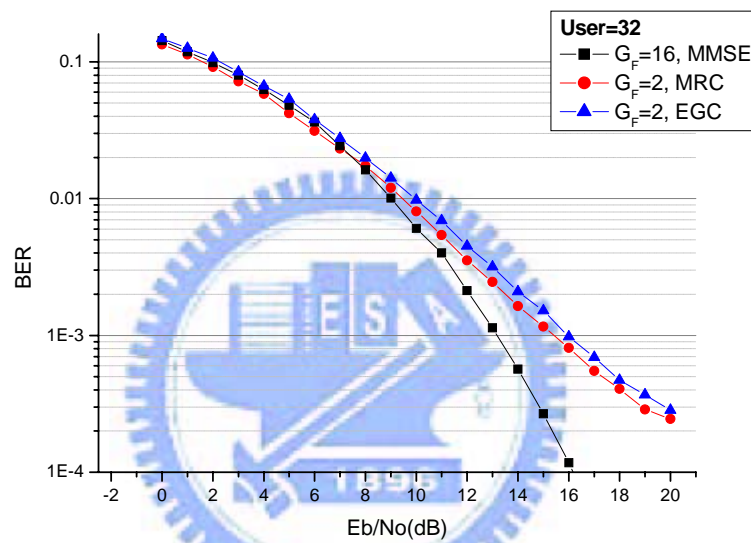


Fig. 4.13 Performance comparison between single user detection with user number = 32

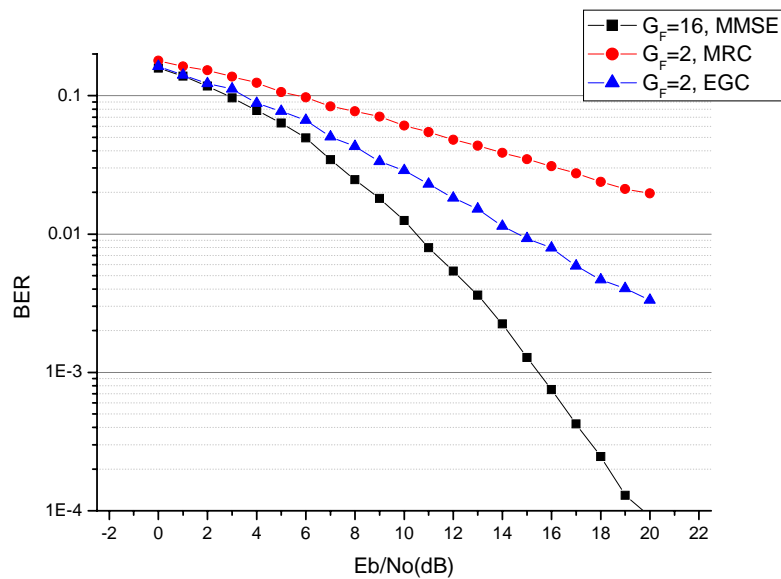
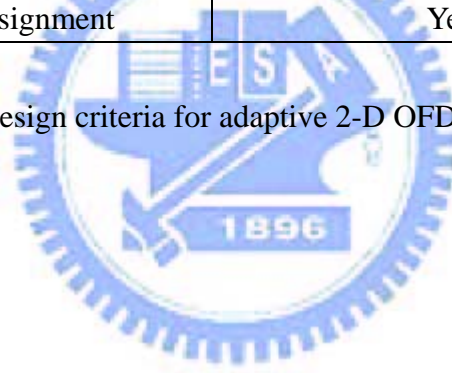


Fig. 4.14 Performance comparison between single user detection with user number = 64

Table 4.1 explains the design criteria for adaptive 2-D OFDM-CDMA systems. According to the performances shown before, the design criteria are separated into two parts based on user number. For light load channel, we suggest that to maintain MAI free has the higher priority than to get largest diversity. Therefore, to make MAI free must choose right length of time and frequency spreading factor according to user number and use MRC scheme with code assignment. For heavy load channel, because it is hard to maintain MAI free, to get the largest diversity and do the best to suppress MAI is the main principle. We choose SF length based on channel coherent bandwidth to get the largest diversity gain, and use MMSEC or multi-user detection to suppress MAI efficiently.

Light load (User number <17)	
Priority	MAI free>Diversity gain
Principle	Under MAI free condition, choose the largest diversity
SF length(G_F G_T) selection	Based on user number
Combining schemes	MRC
Code assignment	Yes
Heavy load (User number >17)	
Priority	Diversity gain >MAI free
Principle	Choose the largest diversity and suppress MAI
SF length(G_F G_T) selection	Based on channel condition
Combining schemes	MMSE or Multi-user detection
Code assignment	Yes

Table 4.1 Design criteria for adaptive 2-D OFDM-CDMA systems



Chapter 5

Multi-user Detection

Many data detection techniques have been proposed for DS-CDMA systems [16]. These algorithms can be divided into single user and multi-user detections. A single-user detector is defined as a receiver structure that requires that no information regarding the other (interfering) users present in the system and demodulates the data signal of one user only. On the contrary, multi-user detection requires the other user's information to help detect the data. Therefore, it has higher complexity but may approach single-user performance. In this chapter we introduce two methods of multi-user detection. The conventional MMSE/PIC detector was first proposed to be used in DS-CDMA systems [16] and recently was suggested to be used in MC-CDMA systems [17]. We propose a new MMSE/PIC multi-user detector for our adaptive 2D OFDM-CDMA systems which has better performance and lower complexity than conventional MMSE/PIC detector for MC-CDMA systems. Considering the demand of low complexity as the single-user detection at receiver side, we propose another multi-user combining method, pre-weight allocation, to perform at the transmitter side.

5.1 MMSE/PIC Multi-user Detection

The single-user detection methods including MRC, EGC and MMSE are introduced in last chapter. In a single-user setting, OFDM-CDMA can exploit all available frequency diversity by employing MRC. In a multi-user setting however, the

capacity of the single-user MRC detector is limited by MAI. The MMSE detector takes into account both MAI and noise and has the best performance. Although this MMSE single-user detector is a good choice, it still suffers from a large performance loss compared to single-user performance. Considering multi-user detection, the maximum-likelihood detector achieves near optimum performance but its complexity increases exponentially with the number of active users. In the DS-CDMA context, suboptimal nonlinear Parallel Interference Cancellation (PIC) schemes have been developed, that cancel out the MAI experienced by each user, based on initial estimates obtained through a matched-filter bank. They feature only linear complexity in the number of active users and show moderate performance loss compared to the optimum detector. However, they generally require a large number of stages. To avoid this, a new multi-user detector for DS-CDMA was recently proposed, that uses an MMSE detector to obtain the initial estimates. Compared to the conventional PIC schemes, it only requires one PIC stage to obtain near optimum performance. The detector consists of three stages: a linear per-carrier MMSE stage, a per-carrier PIC stage and finally still a MMSE per-carrier stage.

In this thesis, considering the conventional multi-carrier based MMSE/PIC multi-user detector is not suited for our 2-D OFDM-CDMA systems, we propose a low complexity MMSE/per-carrier PIC multi-user detector for 2-D OFDM-CDMA systems.

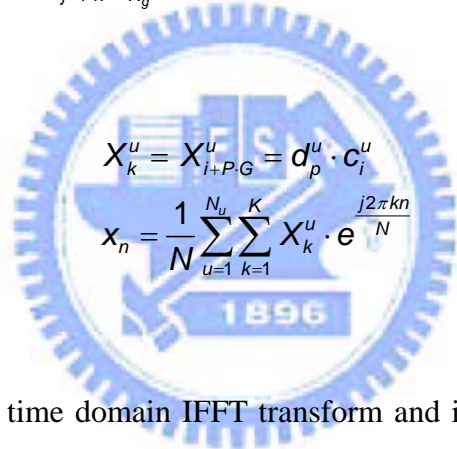
5.1.1 Conventional 1-D MMSE/PIC Detector

In the beginning, we introduce the 1-D MC-CDMA system [18], and then explain the multi-user receiver.

The transmitted MC-CDMA symbols are generated by spreading the original data stream over the different sub-carriers with a frequency spreading factor. The transmitted symbols are

$$s(t) = \sum_{j=1}^{\infty} \sum_{n=-N_g}^{N-1} x_n \cdot g_T(t - nT_s - jN_{OFDM}T_s) \quad (5.1)$$

Where



$$\begin{aligned} X_k^u &= X_{i+P.G}^u = d_p^u \cdot c_i^u \\ x_n &= \frac{1}{N} \sum_{u=1}^{N_u} \sum_{k=1}^K X_k^u \cdot e^{j\frac{2\pi kn}{N}} \end{aligned} \quad (5.2)$$

After frequency to time domain IFFT transform and inserting the cyclic prefix, the parallel to serial converted MC-CDMA time domain symbols are transmitted over the channel. In the receiver side, the received symbols are serial to parallel converted and the cyclic prefix is removed. The received signals are

$$\begin{aligned} r(t) &= s(t) \otimes h(t) \otimes g_R(t) + n(t) \otimes g_R(t) \\ &= \sum_{j=1}^{G_T} \sum_{n=-N_g}^{N-1} x_{n,j} f(t - nT_s - jN_{OFDM}T_s) + z(t) \end{aligned} \quad (5.3)$$

* $f(t) = g_T(t) \otimes h(t) \otimes g_R(t)$: Overall Impulse Response

* $z(t) = n(t) \otimes g_R(t)$

And after sampling the received signal, the signal becomes

$$\begin{aligned}
 r(n, j) &= r(t) \Big|_{t=nT_s + jN_{OFCDM}T} \\
 &= y(n, j) + z(n, j) \quad n = 0, \dots, N-1
 \end{aligned} \tag{5.4}$$

Then performing the FFT to obtain the data in the frequency domain

$$\begin{aligned}
 Y(k, j) &= DFT \{y(n, j)\} \quad k = 0, \dots, N-1 \\
 &= \sum_{n=0}^{N-1} y_{n,j} e^{-j2\pi kn/N} \\
 &= \sum_{n=0}^{N-1} \left[\frac{1}{N} \sum_{u=1}^{N_u} \sum_{k=0}^{N-1} X_{k,j}^u H_{k,j} \cdot e^{j2\pi kn/N} \right] \cdot e^{-j2\pi kn/N} \\
 &= \sum_{u=1}^{N_u} \sum_{k=0}^{N-1} X_{k,j}^u H_{k,j} \\
 &= \sum_{u=1}^{N_u} \sum_{p=0}^{P-1} \sum_{i=0}^{G-1} d_p^u \cdot c_i^u \cdot H_{i+pG,j}
 \end{aligned} \tag{5.5}$$

Following FFT modulation, multi-user detection is performed as Fig. 5.1

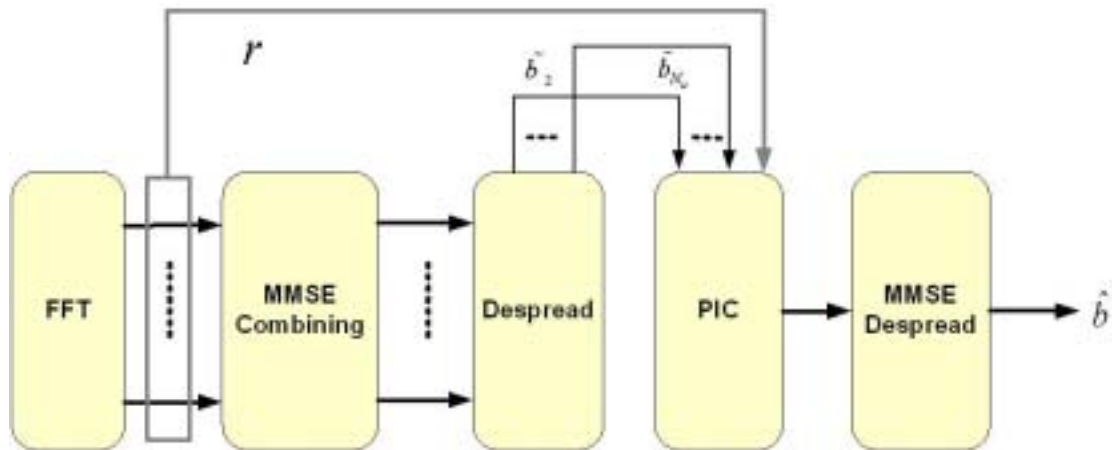


Fig. 5.1 MMSE/PIC multi-user detector for MC-CDMA systems

The combined MMSE/PIC detector consists of three stages: a linear per-carrier MMSE stage, a per-carrier PIC and followed with MMSE stage. The first stage produces initial bit estimates of all user, that are used by the second stage to cancel on a per-carrier basis the interference experienced by each user. Finally, the MMSE combines the cleaned-up signals over the carriers to produce the final bit estimates. Then we introduce the each stage in detail.

First stage: MMSE multi-user detector

The first stage is a linear filter bank whose coefficients are determined according to an MMSE criterion. The optimization criterion is to find for each sub-carrier i (We can omit the subscription p without loss of generality.), a filter coefficient W_i that multiplies the observation r_i such that,

$$W_i = \arg \min_{W_i} E \left\{ |D_i - W_i \cdot r_i|^2 \right\} \quad (5.6)$$

The combining weight for the i th sub-carrier symbol is obtained by applying the orthogonality principle,

$$W_i = \frac{H_i^*}{|H_i|^2 + \frac{\sigma_n^2}{N_u \cdot P_c}} \quad (5.7)$$

Finally, the initial data vector estimate for user u is given by

$$\tilde{b}^u = \text{sgn} \left[\sum_{i=1}^G r_i \cdot W_i \cdot c_i^u \right] \quad (5.8)$$

where $u = 2, 3, \dots, N_u$ and assume user1 is the desired user

Second stage: Parallel Interference Cancellation

As initial estimates, it uses the estimate data from MMSE detector stage. To obtain the estimate MAI, the estimate data is multiplied by the spreading code and the complex fading gain. After combining the other user's MAI, the total MAI is subtracted by the received signal. The resulting signal for user 1 after cancellation is,

$$\tilde{r}_i = r_i - \sum_{u=2}^{N_u} H_i \cdot \tilde{b}^u \cdot c_i^u \quad (5.9)$$

Third stage: MMSE multi-user detector

The final bit estimate for user 1(desired user) is obtained by also applying MMSE to the signal of user 1 after cancellation.

$$\hat{b}^1 = \text{sgn} \left[\sum_{i=1}^G \tilde{r}_i \cdot W_i \cdot c_i^1 \right] \quad (5.10)$$

5.1.2 Low Complexity 2-D MMSE/PIC Detector

For our 2D OFDM-CDMA systems, we find that the 1-D MMSE/PIC multi-user detector is not suitable for use. This is because the distribution of MAI in 2-D OFDM-CDMA systems is different from that in 1-D systems based on the joint consideration of code assignment issue, the selection of SF patterns and sub-carrier allocation. For example, the generation of MAI is explained in the Fig.3-5 in Chapter 3. MAI is formed just due to the selection of the identical time domain spreading codes between different users in the 2-D architecture. However, it is not true for 1-D

system because any other user would cause MAI for the desired user.

MAI cancellation is the purpose of the multi-user detection. Therefore, it is unnecessary to cancel the user's data corresponding to MAI free with the desired user. Moreover, we can say that it is forbidden to cancel these users' data. This is because to detect these users' data not only bring no benefit but cause additional MAI. Fig.5.2 shows different desired users and their corresponding MAI users. For example, if user 1 who uses code 1 is the desired user, the only interference is from user 5. We just need to estimate the data of user 5 and cancel it. But if we estimate and cancel all other users' data according the principle of 1-D MMSE/PIC detector, the BER performance becomes worse due to additional MAI as the block diagrams shows on the right side of Fig.5.2. To avoid canceling the incorrect MAI, we don't need to make effort to estimate the data of user number = 2, 3, 4, 6, 7, 8. As a result, we can obtain a low complexity 2-D MMSE/PIC detector.

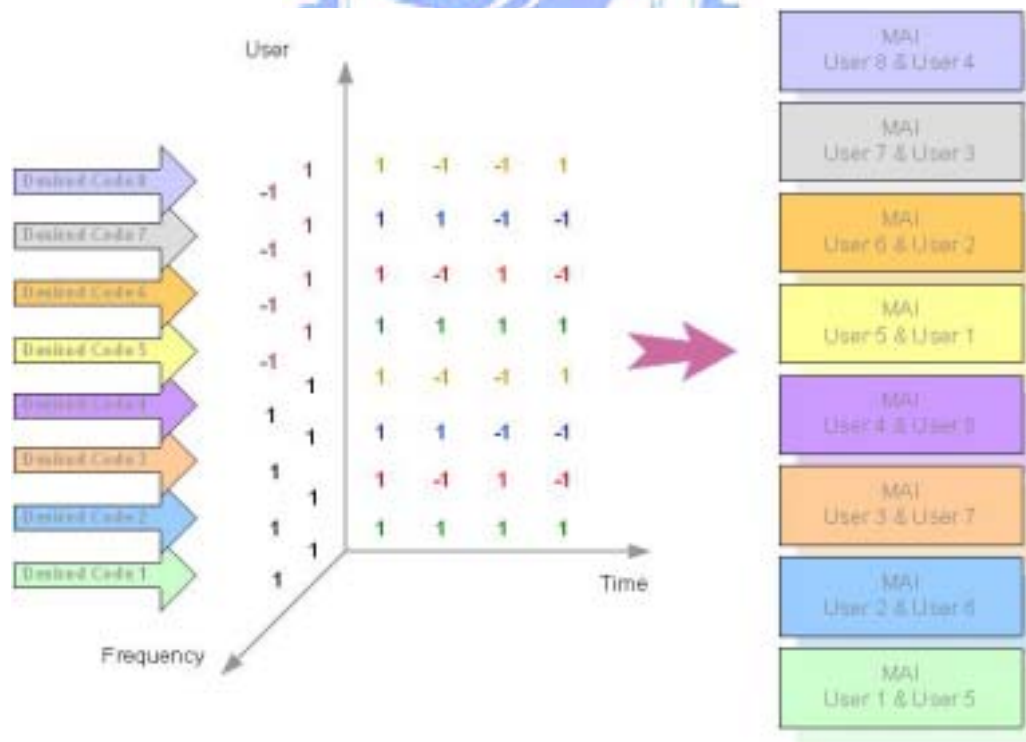


Fig. 5.2 The relation between desired user and MAI users

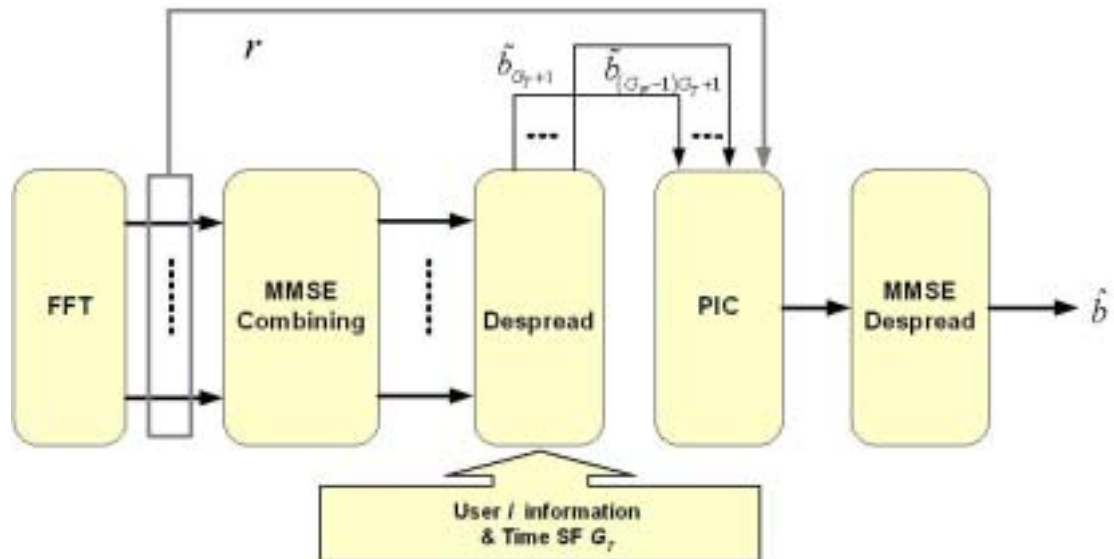


Fig. 5.3 Proposed low complexity MMSE/PIC detector for 2-D OFDM-CDMA systems

Fig. 5.3 shows the architecture of 2-D MMSE/PIC detector. We don't need to estimate all the users' data but just need to estimate the users with the same time domain spreading codes. This is the mainly difference between 1-D and 2-D detector.

First stage: MMSE multi-user detector

In the first stage we still use an MMSE criterion to find the combining weights which satisfy,

$$W_{i,j} = \arg \min_{W_{i,j}} E \left\{ \left| D_{i,j} - W_{i,j} \cdot r_{i,j} \right|^2 \right\} \quad (5.11)$$

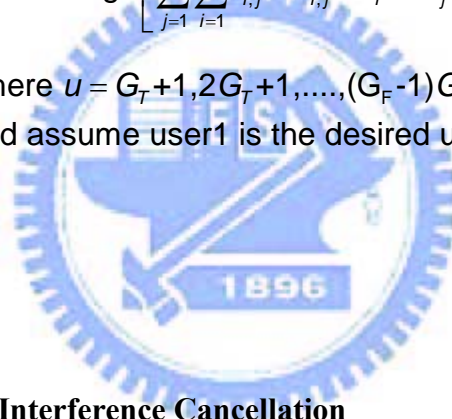
The combining weight for the i th sub-carrier of the j th OFDM symbol is

$$W_{i,j} = \frac{H_{i,j}^*}{\left| H_{i,j} \right|^2 + \frac{\sigma_n^2}{N_u \cdot P_c}} \quad (5.12)$$

Finally, the data vector estimate for user u is given by

$$\hat{b}^u = \text{sgn} \left[\sum_{j=1}^{G_T} \sum_{i=1}^{G_F} r_{i,j} \cdot W_{i,j} \cdot c f_i^u \cdot c t_j^u \right] \quad (5.13)$$

where $u = G_T+1, 2G_T+1, \dots, (G_F-1)G_T+1$
and assume user1 is the desired user



Second stage: Parallel Interference Cancellation

As initial estimates, it uses the estimate data from MMSE detector stage. To obtain the estimate MAI, the estimate data is multiplied by the spreading code and the complex fading gain. After combining the other user's MAI, the total MAI is subtracted by the received signal. The resulting signal for user 1 after cancellation is,

$$\tilde{r}_i = r_i - \sum_{u=G_T+1}^{(G_F-1)G_T+1} H_i \cdot \tilde{b}^u \cdot c_i^u \quad (5.14)$$

Third stage: MMSE multi-user detector

The final bit estimate for user 1(desired user) is obtained by also applying MMSE to the signal of user 1 after cancellation.

$$\hat{b}^1 = \text{sgn} \left[\sum_{i=1}^G \tilde{r}_i \cdot W_i \cdot c_i^1 \right] \quad (5.15)$$

Fig. 5.4 shows the performance comparisons between MMSE sing-user detector and proposed MMSE/PIC multi-user detector. The curve $G_F = 16$ has the best performance and it also has lower complexity than $G_F = 64$ (MC-CDMA). The performance of $G_F = 16$ with MMSE/PIC detector is better than MMSE detector by 3dB gain.

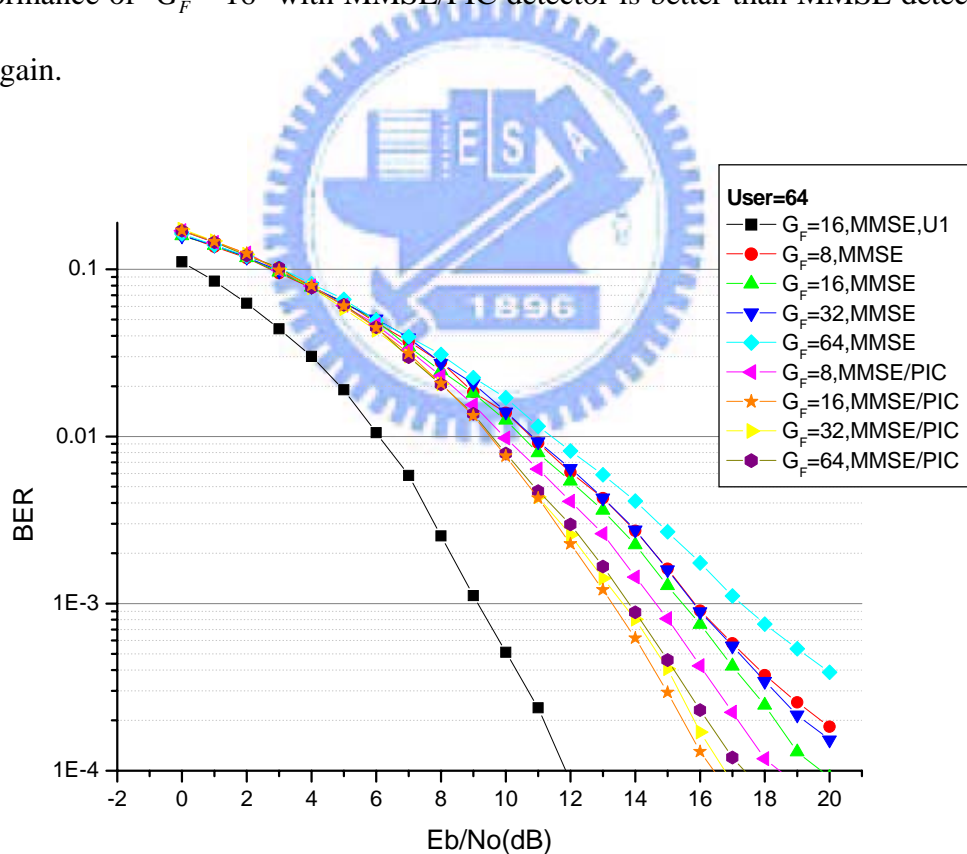


Fig. 5.4 Performance comparisons between MMSE and MMSE/PIC detector

5.2 Combined Pre-Weight Processing/MMSE Detector

We introduce the MMSE/PIC multi-user detector in the last section. Although the complexity of proposed 2-D MMSE/PIC detector is lower than conventional 1-D detector, but it still higher than single-user detection. Therefore, we proposed another method which combined pre-weight processing at transmitter side and MMSE single-user detector at receiver side to move the complexity from receiver to transmitter side.

The objective of pre-weight processing is to find out optimal pre-weights of each user to minimize combining MSE while MMSE method is applied at receiver side [18-19]. At first, we introduce pre-weight processing/MMSE detector for the MC-CDMA system and then propose pre-weight processing/MMSE detector for 2-D OFDM-CDMA systems.

5.2.1 1-D Pre-Weight Processing/MMSE Detector[20]

Fig.5.5 is the transmitter structure for MC-CDMA systems. The difference between this structure and original MC-CDMA systems is adding the pre-weight processing on each sub-carrier. Fig.5.6 shows the receiver with MMSE detector for MC-CDMA systems.

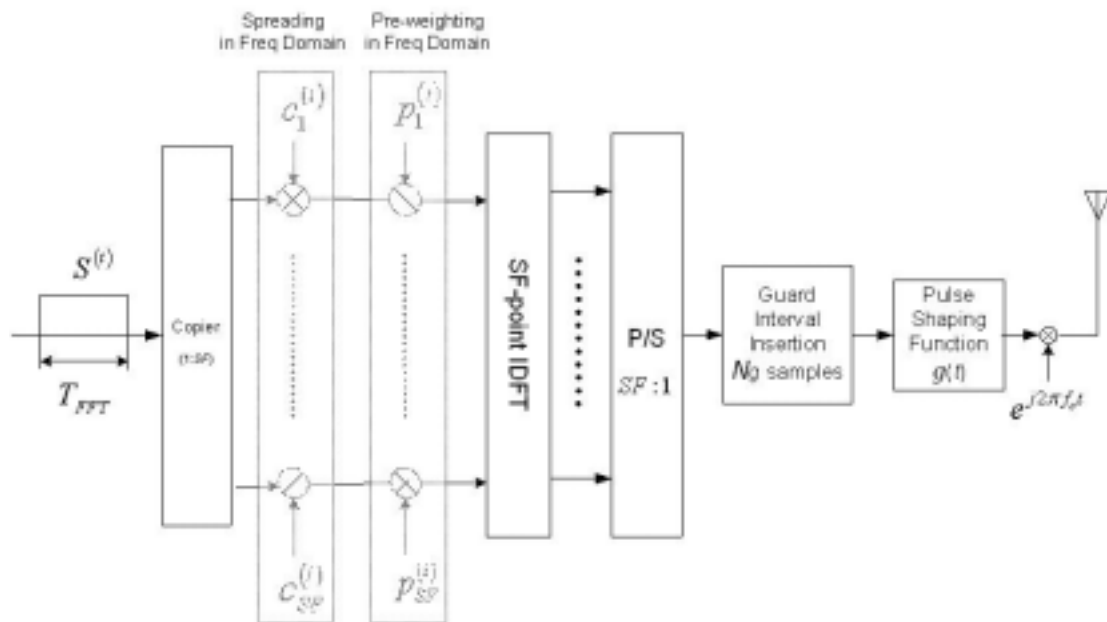


Fig.5.5 Combined pre-weight processing/MMSE transmitter architecture for MC-CDMA system

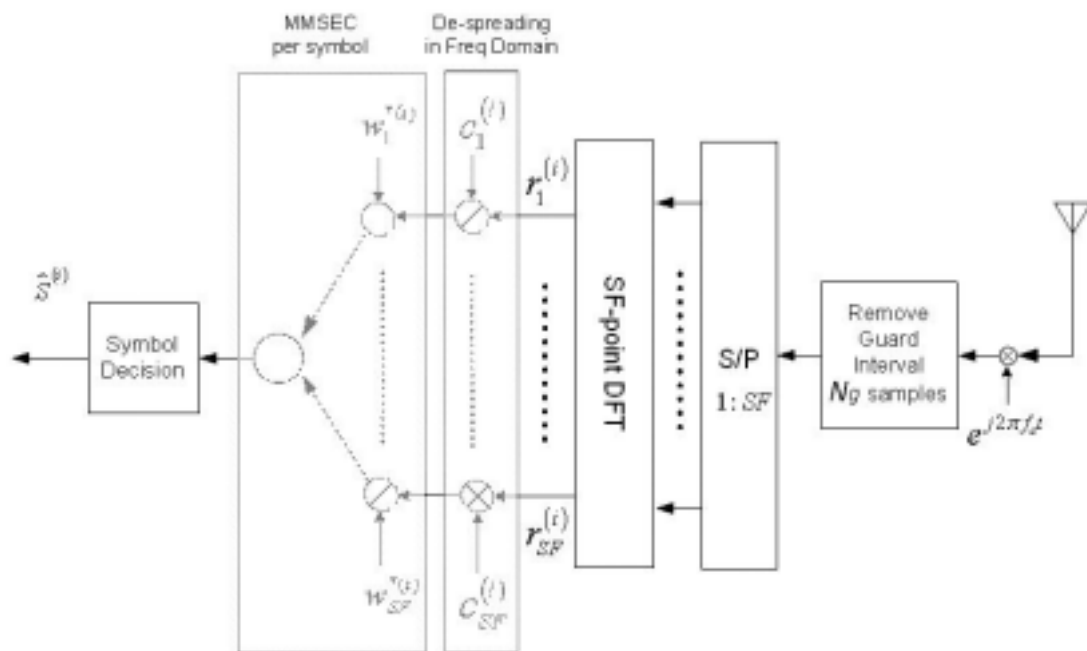
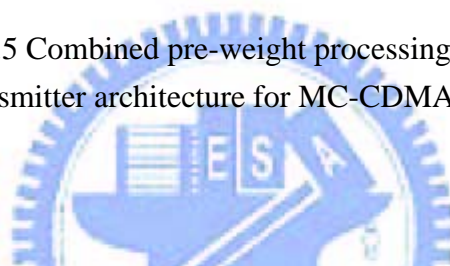


Fig.5.6 Combined pre-weight processing/MMSE receiver architecture for MC-CDMA system

Then we explain how to obtain the pre-weight vector for each user assuming the channel condition and user spreading codes are known. The received signal after FFT is

$$r_k^{(i)} = \left(\sum_{i'=1}^{N_u} S^{(i')} p_k^{(i')} c_k^{(i')} \right) H_k^{(i)} + N_k^{(i)}, \quad k = 1, \dots, SF \quad i = 1, \dots, N_u \quad (5.16)$$

We want the received signals after combining and despreading could approximate the transmit data, which means

$$\begin{aligned} \frac{1}{SF} \sum_{k=1}^{SF} r_k^{(i)} c_k^{(i)} w_k^{*(i)} &\rightarrow S^{(i)} \\ \frac{1}{SF} \overline{w^{(i)}}^H \overline{rc^{(i)}} &\rightarrow S^{(i)}, \quad \overline{w^{(i)}} = [w_1^{(i)}, \dots, w_{SF}^{(i)}]^T, \quad \overline{rc^{(i)}} = [r_1^{(i)} c_1^{(i)}, \dots, r_{SF}^{(i)} c_{SF}^{(i)}]^T \end{aligned} \quad (5.17)$$

Next we apply MMSE criterion to obtain the combining weights

$$\begin{aligned} \min E \left[\left| \frac{1}{SF} \overline{w^{(i)}}^H \overline{rc^{(i)}} - S^{(i)} \right|^2 \right] \\ \therefore \frac{1}{SF} \overline{w^{(i)}} = \left\{ E \left[\overline{rc^{(i)}} \overline{rc^{(i)}}^H \right] \right\}^{-1} \cdot E \left[\overline{rc^{(i)}} S^{*(i)} \right] = R_{rc^{(i)}}^{-1} \cdot \sigma_s^2 \cdot \overline{Hp^{(i)}}, \end{aligned} \quad (5.18)$$

Then

$$\begin{aligned}
MMSE &= E \left[\left| \sigma_s^2 \cdot \overline{Hp}^{(i)H} \left(R_{rc}^{-1} \right)^H rc^{(i)} - S^{(i)} \right|^2 \right] \\
&= (\sigma_s^2)^2 E \left[\left| \overline{Hp}^{(i)H} R_{rc}^{-1} rc^{(i)} \right|^2 \right] - 2 \operatorname{Re} \left\{ E \left[\sigma_s^2 \overline{Hp}^{(i)H} R_{rc}^{-1} rc^{(i)} S^{*(i)} \right] \right\} + \sigma_s^2 \\
&= (\sigma_s^2)^2 \overline{Hp}^{(i)H} R_{rc}^{-1} \overline{Hp}^{(i)} - 2 (\sigma_s^2)^2 \operatorname{Re} \left\{ \overline{Hp}^{(i)H} R_{rc}^{-1} \overline{Hp}^{(i)} \right\} + \sigma_s^2 \quad (5.19) \\
&= \sigma_s^2 - (\sigma_s^2)^2 \overline{Hp}^{(i)H} R_{rc}^{-1} \overline{Hp}^{(i)}
\end{aligned}$$

where $\overline{Hp}^{(i)} = [H_1^{(i)} p_1^{(i)}, \dots, H_{SF}^{(i)} p_{SF}^{(i)}]^T$,

$$R_{rc}^{-1} = E \left[rc^{(i)} rc^{(i)H} \right],$$

$$rc^{(i)} = [r_1^{(i)} c_1^{(i)}, \dots, r_{SF}^{(i)} c_{SF}^{(i)}]^T$$

And after analyzing the R_{rc}^{-1} , we get

$$MMSE = \sigma_s^2 - (\sigma_s^2)^2 \cdot \frac{\overline{p}^{(i)H} H^{(i)H} \left(\sigma_N^2 I_{SF} + \sigma_s^2 \sum_{\substack{i'=1 \\ i' \neq i}}^{Nu} \overline{H}^{(i)(i')} \overline{H}^{(i)(i')H} \right)^{-1} H^{(i)} \overline{p}^{(i)}}{1 + \sigma_s^2 \overline{p}^{(i)H} H^{(i)H} \left(\sigma_N^2 I_{SF} + \sigma_s^2 \sum_{\substack{i'=1 \\ i' \neq i}}^{Nu} \overline{H}^{(i)(i')} \overline{H}^{(i)(i')H} \right)^{-1} H^{(i)} \overline{p}^{(i)}} \quad (5.20)$$

We want to minimize the MMSE by choosing $\overline{p}^{(i)}$, and it is equivalent to maximize

$$\overline{p}^{(i)H} H^{(i)H} \left(\sigma_N^2 I_{SF} + \sigma_s^2 \sum_{\substack{i'=1 \\ i' \neq i}}^{Nu} \overline{H}^{(i)(i')} \overline{H}^{(i)(i')H} \right)^{-1} H^{(i)} \overline{p}^{(i)} \quad (5.21)$$

Finally, we find $\overline{p}^{(i)}$ equals the largest eigenvalue corresponding to the eigenvector of

$$H^{(i)H} \left(\sigma_N^2 I_{SF} + \sigma_s^2 \sum_{\substack{i'=1 \\ i' \neq i}}^{Nu} \overline{H}^{(i)(i')} \overline{H}^{(i)(i')H} \right)^{-1} H^{(i)} \quad (5.22)$$

Because we hope the total performance reaches the best, which means to minimize the sum of mean square error of each user, we should decide the pre-weight vectors with joint optimization method. As a result, next we introduce the search algorithm to iterative update the user's pre-weight vectors.

Pre-weight vectors update algorithm:

- Step 1: Initially set uniform allocation for all users, namely

$$\overline{p}_0^{(1)} = \overline{p}_0^{(2)} = \dots = \overline{p}_0^{(SF)} = [1 \ 1 \ \dots \ 1]_{1*SF}^T$$

, and compute sum of all users ' MMSE Sum_0 ,

and set k=0.

- Step 2: Update one user ' s pre-weight vector once using the method

mentioned above.

$$\left[\overline{p}_k^{(1)} \ \overline{p}_k^{(2)} \ \dots \ \overline{p}_k^{(SF)} \right] \text{ and compute corresponding } Sum_{k+1}^1$$

$$\left[\overline{p}_k^{(1)} \ \overline{p}_k^{(2)} \ \dots \ \overline{p}_k^{(SF)} \right] \text{ and compute corresponding } Sum_{k+1}^2$$

⋮

$$\left[\overline{p}_k^{(1)} \ \overline{p}_k^{(2)} \ \dots \ \overline{p}_k^{(SF)} \right] \text{ and compute corresponding } Sum_{k+1}^{SF}$$

– Step 3: Select the smallest one among

$$Sum_{k+1}^j, j=1,2,\dots,SF$$

$$, \text{ namely } Sum_{k+1}^i = \min\left(Sum_{k+1}^1 \quad Sum_{k+1}^2 \quad \dots \quad Sum_{k+1}^{SF}\right)$$

If $Sum_{k+1}^i \geq Sum_k$, stop. Then $\left[\overline{p_k^{(1)}} \quad \overline{p_k^{(2)}} \quad \dots \quad \overline{p_k^{(SF)}}\right]$ and Sum_k are the final solution.

If $Sum_{k+1}^i < Sum_k$, then set $Sum_{k+1} = Sum_{k+1}^i$,

$$\left[\overline{p_{k+1}^{(1)}} \quad \overline{p_{k+1}^{(2)}} \quad \dots \quad \overline{p_{k+1}^{(SF)}}\right] = \left[\overline{p_k^{(1)}} \quad \dots \quad \overline{p_k^{(i)'}} \quad \dots \quad \overline{p_k^{(SF)}}\right],$$

$k=k+1$ and return to step 2.

5.2.2 2-D Pre-Weight Processing/MMSE Detector

Referring to the combined pre-weight processing/MMSE scheme used in MC-CDMA systems, we take this algorithm for 2-D OFDM-CDMA systems. The most part including the pre-weight vectors and the search method is the same with 1-D detector. The different part is similar to 2-D MMSE/PIC detector as mentioned before. Because MAI appears just when some users use the same time domain spreading code with the desired user. That is, we don't need to process all the simultaneous users but just only need to calculate the pre-weight vectors with the same time spreading codes. Observing the equation (5.22), the complexity is very high to obtain the result for full user number. But when we use it for 2-D system, the complexity reduces quite substantially. Moreover, Fig.5.7 shows the curve $G_F = 16$ has better performance than $G_F = 64$ (MC-CDMA).

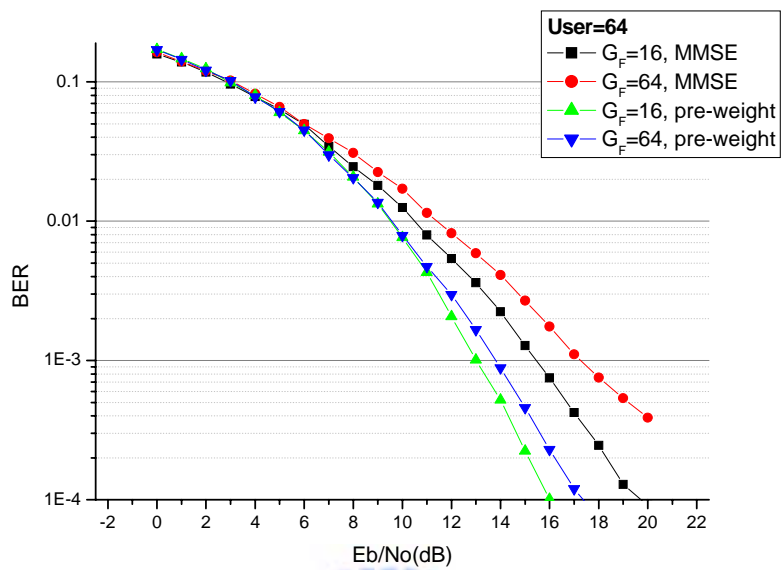
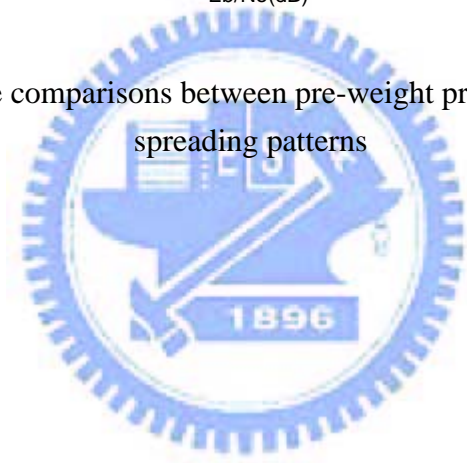


Fig.5.7 Performance comparisons between pre-weight processing with different spreading patterns



Chapter 6

Conclusion

In this thesis, we propose an adaptive OFDM-CDMA system with time and frequency domain spreading for the forward link. We take many design issues into account at the same time including the combinations of time and frequency spreading patterns, sub-carrier allocation methods, spreading code assignment for simultaneous users, and the diversity combining schemes employed in the receiver side.

Because the system performance depends mainly on the tradeoff relation between the diversity gain and the MAI loss, our research is focused on the jointly controlling all the factors to balance the diversity and MAI based on the known channel conditions and simultaneous user number. We find that there are two directions to achieve the objective: one is to maximize the diversity under the MAI free condition, and the other is to find the largest diversity and use complex detectors to suppress MAI.

For multi-user detection, we propose two new schemes for 2-D OFDM-CDMA systems: one is MMSE/PIC at receiver side and the other is Pre-weight processing at transmitter side. Both of these two methods have lower complexity because not all users but just the users who have identical time spreading codes with the desired user need to be canceled. Furthermore, the better performance is achieved than 1-D multi-user detectors.

According to the simulation results, we suggest that the low complexity detector such as MRC single user detector with code assignment is a good choice for the light load. On the other hand, when the user number increases, the best way is to maximize the diversity and use MMSE or multi-user detector to suppress MAI.



References

- [1] 3GPP, 3G TR25.858, "Physical Layer Aspects of UTRA High Speed Downlink Packet Access".
- [2] M. Sawahashi, K. Higuchi, S. Tanaka and F. Adachi, "Enhanced wireless access technologies and experiments for W-CDMA communications", *IEEE personal Commun.*, vol. 7, no. 6, Dec. 2000, pp. 6-17.
- [3] S. Hara, and R. Prasad, "Overview of Multicarrier CDMA," *IEEE Commun. Mag.*, vol. 32, no. 12, Dec. 1997, pp. 126-133.
- [4] S. Hara, and R. Prasad, "Design and performance of multi-carrier CDMA system in frequency-selective Rayleigh fading channels," *IEEE Transactions on Vehicular Technology*, vol. 48, no. 5, Dec. 1999, pp. 1584-1595.
- [5] N. Yee, J.-P. Linnartz, and G. Fettweis, "Multi-carrier CDMA in indoor wireless radio networks," in *Proc. IEEE PIMRC'93*, Sept. 1993, pp. 109-113
- [6] A. Persson, T. Ottosson, and E. Strom, "Time-frequency localized CDMA for downlink multi-carrier systems," in *Proc. of IEEE ISSSTA'02*, Sept. 2002, pp. 118-122
- [7] Lie-Liang Yang and Lajos Hanzo, "Multicarrier DS-SS-CDMA: A multiple access scheme for ubiquitous broadband wireless communications," *IEEE Commun. Mag.*, vol. 41, no. 10, Oct. 2003, pp. 116-124.
- [8] Lei Xiao, "A novel MC-2D-SS-CDMA communication systems and its detection methods," in *Proc. of IEEE ICC'00*, June 2000, pp. 1223-1227.
- [9] A. Matsumoto, K. Miyoshi, M. Uesugi, O. Kato, "A study on time domain spreading for OFSS-CDMA," in *Proc. of Wireless Personal Multimedia Communications*, Oct. 2002, pp. 725-728.
- [10] N. Maeda, Y. Kishiyama, H. Atarashi, and M. Sawahashi, "Broadband packet wireless access based on VSF-OFSS-CDMA and MC/SS-CDMA," in *Proc. of IEEE PIMRC'02*, Sept. 2002, pp. 992-997.
- [11] N. Maeda, Y. Kishiyama, H. Atarashi, and M. Sawahashi, "Throughput comparison between VSF-OFSS-CDMA and OFDM considering effect of sectorization in forward link broadband packet wireless access," in *Proc. of IEEE VTC'02*, Sept. 2002, pp. 47-51.

- [12] N. Maeda, Y. Kishiyama, H. Atarashi, and M. Sawahashi, "Variable spreading factor – OFCDM with two dimensional spreading that prioritizes time domain spreading for forward link broadband wireless access," in *Proc. of IEEE VTC'03*, May 2003, pp. 127-132.
- [13] A. Pandharipande, "Principles of OFDM", in *Potentials of IEEE*, Vol. 21, Issue: 2, April-May, 2002, pp.16 -19
- [14] Thit Minn, Kai-Yeung Siu, "Dynamic Assignment of Orthogonal Variable-Spreading –Factor Codes in W-CDMA", in *IEEE Journal*, Vol.18, Issue:8, Aug 2000, pp. 1429-1440
- [15] M. Noriyuki, H. Atarashi, and M. Sawahashi, "Performance Comparison of Channel Interleaving Methods in Frequency Domain for VSF-OFCDM Broadband Wireless Access in Forward Link" in *IEICE Trans.* Vol. E86-B, No. 1, Jan 2003, pp.55-60
- [16] D. Koulakiotis, A.H. Aghvami, "Data Detection Techniques for DS/CDMA Mobile Systems : A Review" in *IEEE Personal Commun.* Vol.7, Issue:3, June 2000, pp. 24-34
- [17] F. Petre, P. Vandenameele, A. Bourdoux, B. Gyselinckx, M.Engels, M. Moonen, H. De Man. "Combined MMSE/pcPIC Multiuser Detection for MC-CDMA" in *Proc. of IEEE VTC2000* Vol.2, 15-18 May 2000 pp.770 - 774
- [18] R. Esmailzadeh and M. Nakagawa, "Pre-rake Diversity Combination for Direct Sequence Spread Spectrum Communications Systems," in *Proc. Of IEEE ICC' 93* May 1993, pp.463-467
- [19] B. R. Vojcic and W.M. Jang, "Transmitter Precoding in Synchronous Multiuser Communications," *IEEE Trans. Commun.*, Oct. 1998, pp. 1346-1355
- [20] Chih-Cheng Kuo, "Design and Performance Analysis of Forward Link Multi-carrier CDMA Systems with Transmitter Pre-weighting Processing" to be published.